Dalton Transactions

Water-dispersible Pd-N-heterocyclic carbene complex immobilized on magnetic nanoparticles as a new heterogeneous catalyst for fluoride-free Hiyama, Suzuki and cyanation reactions in aqueous media

Journal:	*Dalton Transactions*
Manuscript ID	Draft
Article Type:	Paper
Date Submitted by the Author:	n/a
Complete List of Authors:	omarzehi Chahkamali, farhad; univ of Birjand Sobhani, Sara; University of Birjand, chemistry Sansano, José; University of Alicante, Organic Chemistry

ARTICLE

Water-dispersible Pd-*N*-heterocyclic carbene complex immobilized on magnetic nanoparticles as a new heterogeneous catalyst for fluoride-free Hiyama, Suzuki and cyanation reactions in aqueous media

Farhad Omarzehi Chahkamali,[a] Sara Sobhani*[a] and José Miguel Sansano[b]

Pd-*N*-heterocyclic carbene complex immobilized on magnetic nanoparticles is synthesized and characterized by different techniques such as FT-IR, XPS, TEM, EDX, FESEM, VSM, TGA and ICP. The synthesized catalyst was used as a new water dispersible heterogeneous catalyst in the fluoride-free Hiyama, Suzuki and cyanation reactions in pure water. By this method, different types of biaryls and aryl nitriles were synthesized in good to high yields by the reaction of a variety of aryl iodides, bromides and chlorides with triethoxyphenylsilane, phenylboronic acid and $K_4[Fe(CN)_6]\cdot 3H_2O$, respectively. The presence of sulfonates as hydrophilic groups on the surface of the catalyst offers a highly water dispersible, active and yet magnetically recoverable Pd catalyst. The possibility to perform the reaction in water as a green medium, easy catalyst recovery and reuse by successive extraction and final magnetic separation, and the absence of any additives or co-solvents make this method as an eco-friendly and economical protocol for the synthesis of biaryl derivatives and aryl nitriles.

Introduction

A plethora of biochemical reactions occurs in aqueous media. Water is inexpensive, non-flammable, and nontoxic, with a high heat capacity.[1,2] Nonetheless, a very small percentage of synthetic organic reactions are carried out in aqueous media. The reasons for the historical restricted use of water as the reaction medium may be related to two main reasons: the first is the hydrophobic effect, which severely limits the solubility of nonpolar organic materials and the second is the instability of organometallic complexes in aqueous media. This important drawback is also the main reason why most of the reactions that are carried out in water include also a co-solvent or phase transfer agent to improve solubility. However, lower solubility of the products in water provides easy product separation. Although, water often considered as the "natural enemy" of organometallic species,[3] Breslow was proposed the first *N*-heterocyclic carbene (NHC) catalysis in the aqueous media.[4] Thermal and chemical stabilities of NHC catalysts in the moisture and air are due to the strong NHC-metal bonds, which originates from strong σ-donor and low σ-acceptor abilities of these ligands. Moreover, the possibility of tuning electronic and steric properties of NHCs adds advantages for the development of novel organometallic materials.[5-10]

Accordingly, NHC-metal complexes have been developed and used widely as suitable and efficient homogeneous catalysts in various organic transformations.[11,12] Despite the wide application of the homogeneous Pd-NHC catalysts in organic transformations, their recycling is very complicated because their separation is extremely difficult.[13,14] One way to overcome this drawback is the immobilization of Pd-NHC on different solid supports such as polystyrene, silica, graphene oxide or magnetic nanoparticles (MNPs).[15-18] Within these solid supports, MNPs provide an easy catalyst isolation by a magnetic separation method using an external magnet. Magnetic separation, which is an alternative to filtration or centrifugation, prevents loss of the catalyst, and saves time and energy.[19-21] However, one significant limitation of using MNPs is that they are readily aggregated when suspended in the solvent due to the self-interactions. Surfactants with relatively high concentrations are often required to prevent such an aggregation in water. A more desirable approach, which avoids using any additives, is

[a] Department of Chemistry, College of Sciences, University of Birjand, Birjand, Iran Fax: +98 56 32202065; Tel: +98 56 32202065; E-mail: ssobhani@birjand.ac.ir, sobhanisara@yahoo.com.
[b] *Departamento de Química Orgánica, Facultad de Ciencias, Centro de Innovación en Química Avanzada (ORFEO-CINQA) and Instituto de Síntesis Orgánica (ISO), Universidad de Alicante, Apdo. 99, 03080-Alicante, Spain.*
Electronic Supplementary Information (ESI) available: [Supplementary information contains NMR spectra of the products].

designing water-dispersible MNPs. This allows reactions to be performed in pure water under near homogeneous conditions. Although preparation of water dispersible MNPs through surface modification with hydrophilic groups have been pursued by many research groups for bio-related applications,[22-24] there are few articles on the synthesis of magnetically recyclable water-dispersible catalysts and their applications in organic transformations in neat water.[25-27] Therefore, there is still much room for developing new magnetically recyclable water-dispersible catalysts in pure aqueous media.

The palladium-catalyzed C–C cross-coupling reactions of aryl halides and organometallic reagents have been developed to produce symmetric and asymmetric biaryl compounds.[28] The biaryl moiety is the core structure of several drugs.[29-31] One of the most common processes for the synthesis of biaryls involves the palladium-catalyzed Hiyama and Suzuki–Miyaura coupling reactions of aryl halides with aryl siloxanes and aryl boronic acids, respectively.[32,33] The notable advantages of using aryl boronic acids and organosilane reagents contrast with the drawbacks of Negishi, Stille, and Kumada–Corriu coupling reactions.[34,35] In Hiyama coupling reactions, organosilanes require fluoride ions for their activation[36,37] or even inorganic bases such as KOH and NaOH in an aqueous solution.[38,39] Both Hiyama and Suzuki cross-coupling reactions in water require the use of organic co-solvents, phase transfer catalysts, surfactants or large amounts of the catalyst.[40-43] More importantly, few examples deal with the most easily available aryl chlorides.[44]

Aryl nitriles are used as building blocks in diverse motifs in agriculture, pharmaceuticals and natural products.[45-47] Apart from the classical methods for the synthesis of aryl nitriles,[48-50] the reaction of aryl halides with cyanating agents in the presence of transition metals as catalysts constitutes an alternative way to prepare aryl nitriles.[51,52] Along this line, cyanation reactions have been reported in the presence of transition metals, using different cyanide reagents such as copper/potassium/sodium and zinc cyanide, trimethylsilyl cyanide, phenyl cyanates, acetone cyanohydrins and benzyl thiocyanates.[53,54] In recent years, potassium hexacyanoferrate (II) trihydrate {$K_4[Fe(CN)_6]\cdot 3H_2O$}, which is a non-hygroscopic, commercially accessible, easily handled and inexpensive cyanide source, has been applied for the cyanation of aryl halides.[55,56] In most cases, the transition metal catalysts are deactivated due to the formation of a stable cyanide complex with transition metals. In-situ generation of cyanide ions from $K_4[Fe(CN)_6]\cdot 3H_2O$ occurs slowly, which improves the efficiency of the metal catalyst.[57]

In our continuous interest in developing the reactions under greener catalyzed conditions,[58-60] herein, we have synthesized a novel water-dispersible Pd-*N*-heterocyclic carbene complex immobilized on magnetic nanoparticles (γ-Fe_2O_3-Pd-NHC-*n*-butyl-SO_3Na, Scheme 1) and characterized it by different methods. We have used this catalyst as a water-dispersible/magnetically recyclable Pd heterogeneous catalyst for C-C (Hiyama, Suzuki and cyanation) reactions in neat water. The presence of nitrogen atoms in NHC ligands was used to incorporate sulfonate salt functionality with hydrophilic character into Pd-NHC supported on MNPs. Hydrophilic character provides dispersion of the catalyst particles in water, which leads to higher catalytic performance and also facile catalyst recovery and reuse.

Experimental section

General information

Chemicals were purchased from Merck Chemical Company. The purity of the products and the progress of the reactions were accomplished by TLC on silica gel polygram SILG/UV254 plates. FT-IR spectra were recorded on a Shimadzu Fourier Transform Infrared Spectrophotometer (FT-IR-8300). The content of Pd in the catalyst was determined by OPTIMA 7300DV ICP analyzer. TEM analysis was performed using TEM microscope (Philips EM 208S). FE-SEM and EDX were obtained using a TSCAN MIRA3. Thermo-gravimetric analysis (TGA) was performed using a Shimadzu thermos-gravimetric analyzer (TG-50). Vibrating Sample Magnetometer (VSM) analysis was performed using VSM (Lake Shore Cryotronics 7407). XPS analyses were performed using a VG-Microteach Multilab 3000 spectrometer, equipped with an Al anode. The deconvolution of spectra was carried out by using Gaussian Lorentzian curves.

Synthesis of imidazole supported on γ-Fe_2O_3 (γ-Fe_2O_3-Im):[61]

The chloro-functionalized γ-Fe_2O_3[62] (1.6 g) was sonicated in dry toluene (30 mL) for 30 min. Imidazole (0.204 g, 3 mmol) was added to the stirring mixture and refluxed for 24 h. After cooling, the mixture was stirred with Et_3N (0.43 mL) for 30 min at room temperature. The solid was separated by an external magnet, washed with H_2O (3 × 10 mL) and acetone (3 × 10 mL) and dried at 70 °C in oven under vacuum.

Synthesis of *n*-butyl sulfonated γ-Fe_2O_3-Im (γ-Fe_2O_3-Im-*n*-butyl-SO_3Na):

The synthesized γ-Fe_2O_3-Im (1.5 g) was sonicated in dry toluene (30 mL) for 30 min. 1,4-Butanesultone (3 mL) was added drop wise to the dispersed mixture and stirred at 90 °C for 24 h. The solid was separated by an external magnet, washed with H_2O (3 × 10 mL) and acetone (3 × 10 mL) and dried at 70 °C in oven under vacuum. The synthesized solid (1.5 g) was sonicated in H_2O (30 mL) for 30 min. NaOAc (4 mmol) was added to the dispersed mixture and stirred for 24 h at room temperature. The solid (γ-Fe_2O_3-Im-*n*-butyl-SO_3Na) was separated by an external magnet, washed with H_2O (3 × 10 mL) and dried at 70 °C in oven under vacuum.

Synthesis of γ-Fe_2O_3- Pd-NHC-*n*-butyl-SO_3Na:

The synthesized γ-Fe_2O_3-Im-*n*-butyl-SO_3Na (1 g) was sonicated in DMSO (15 mL) for 30 min. $Pd(OAc)_2$ (0.5 mmol) was added to the dispersed mixture under N_2 atmosphere at room temperature. The mixture was stirred for 6 h at 50 °C and then allowed to proceed for an additional 4 h at 100 °C. The resulting complex was collected by an external permanent magnet and washed with acetone (3 × 10 mL) and EtOH (3 × 10 mL) to remove the unreacted $Pd(OAc)_2$. The catalyst was obtained as dark-brown solid after drying at 70 °C in oven under vacuum.

Synthesis of γ-Fe_2O_3-Im-Me:

The synthesized γ-Fe_2O_3-Im (1 g) was sonicated in dry toluene (30 mL) for 30 min. Methyl iodide (4 mmol) was added to the dispersed mixture and refluxed for 24 h. The solid was separated by an external magnet, washed with Et_2O (3 × 10 mL) and acetone (3 × 10 mL) and dried in oven under vacuum.

Synthesis of γ-Fe_2O_3-Pd-NHC-Me:

The synthesized γ-Fe_2O_3-Im-Me (1 g) was sonicated in DMSO (15 mL) for 30 min. $Pd(OAc)_2$ (0.5 mmol) was added to the dispersed mixture under N_2 atmosphere at room temperature. The mixture was stirred for 6 h at 50 °C and then allowed to proceed for an additional 4 h at 100 °C. The solid was separated by an external magnet, washed with Et_2O (3 × 10 mL), acetone (3 × 10 mL) and dried at 70 °C in oven under vacuum.

General procedure for Hiyama cross-coupling reaction

γ-Fe_2O_3-Pd-NHC-*n*-butyl-SO_3Na (0.08 or 0.16 mol% based on Pd) was added to a mixture of aryl halide (1 mmol), triethoxyphenylsilane (1.2 mmol) and NaOH (2 mmol) in water (4 mL) and stirred at 80 °C. The progress of the reaction was monitored by TLC. After completion of the reaction, the crude product was extracted using ethyl acetate (3×5 mL). The combined organic layer was then dried over anhydrous Na_2SO_4. After evaporation of solvent, the pure products (**1-6**) were obtained by column chromatography on silica gel eluted with *n*-hexane: EtOAc = 30:1. The aqueous phase, which contains the catalyst, was used for another run.

General procedure for Suzuki-Miyaura cross-coupling reaction

γ-Fe_2O_3- Pd-NHC-*n*-butyl-SO_3Na (0.08 or 0.16 mol% based on Pd) was added to a mixture of aryl halide (1 mmol), phenylboronic acid (1.2 mmol) and K_2CO_3 (2 mmol) in water (4 mL) and stirred at room temperature. The progress of the reaction was monitored by TLC. After completion of the reaction, the crude product was extracted using ethyl acetate (3 × 5 mL). The combined organic layer was then dried over anhydrous Na_2SO_4. After evaporation of solvent, the pure products (**1-6**) were obtained by column chromatography on silica gel eluted with *n*-hexane: EtOAc = 30:1. The aqueous phase, which contains the catalyst, was used for another run.

General procedure for the cyanation reaction of aryl halides

γ-Fe_2O_3-Pd-NHC-*n*-butyl-SO_3Na (0.2 or 0.3 mol% based on Pd) was added to a mixture of aryl halide (1 mmol), $K_4[Fe(CN)_6]\cdot 3H_2O$ (1.2 mmol) and Et_3N (4 mmol) in water (6 mL) and stirred at 90 °C. The progress of the reaction was monitored by TLC. After completion of the reaction, the crude product was extracted using ethyl acetate (3 × 5 mL). The combined organic layer was then dried over anhydrous Na_2SO_4. After evaporation of the solvent, the pure products (**7-15**) were obtained by column chromatography on silica gel eluted with *n*-hexane: EtOAc = 6:1. The aqueous phase, which contains the catalyst, was used for another run.

Results and discussion

Synthesis and characterization of γ-Fe_2O_3-Pd-NHC-*n*-butyl-SO_3Na

Scheme 1 describes the synthetic procedure for the preparation of γ-Fe_2O_3-Pd-NHC-*n*-butyl-SO_3Na. At first, γ-Fe_2O_3 was functionalized by 3-chlorotriethoxypropylsilane and reacted with imidazole. After neutralization with Et_3N, MNPs immobilized with imidazole (γ-Fe_2O_3-Im) was obtained. Reaction of γ-Fe_2O_3-Im with 1,4-butanesultone followed by the treatment with NaOAc, produced

hydrophilic imidazole supported on MNPs (γ-Fe_2O_3-Im-*n*-butyl-SO_3Na). Finally, γ-Fe_2O_3-Pd-NHC-*n*-butyl-SO_3Na was obtained from the reaction of γ-Fe_2O_3-Im-*n*-butyl-SO_3Na with $Pd(OAc)_2$. The presence of hydrophilic sulfonate groups in γ-Fe_2O_3-Pd-NHC-*n*-butyl-SO_3Na makes this compound a hydrophilic material in the aqueous phase without any affinity to the organic phase.

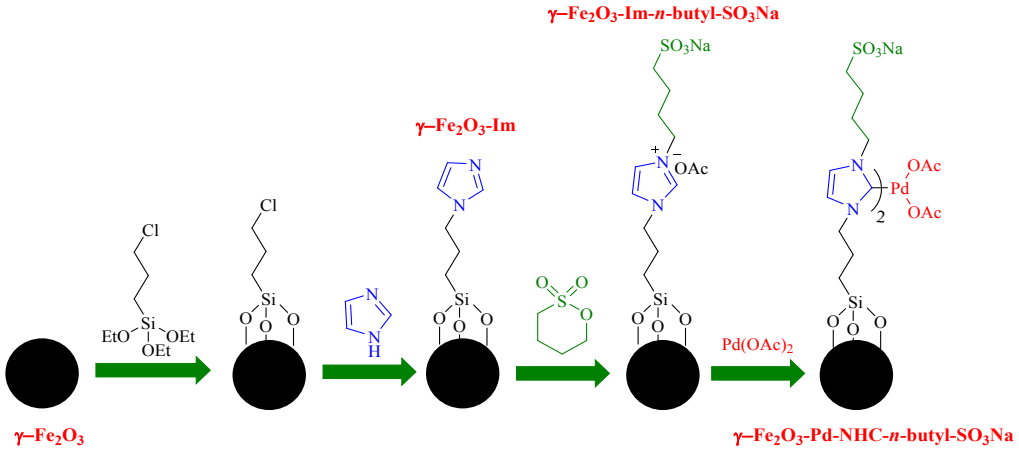

Scheme 1. Synthesis of γ-Fe_2O_3-Pd-NHC-*n*-butyl-SO_3Na

The newly synthesized catalyst was characterized by different techniques. Figure 1 demonstrates FT-IR spectra of γ-Fe_2O_3-Im, γ-Fe_2O_3-Im-*n*-butyl-SO_3Na and γ-Fe_2O_3-Pd-NHC-*n*-butyl-SO_3Na. These spectra exhibited a peak at around 555-676 cm^{-1}, which is attributed to Fe–O stretching vibrations. The bands at around 1068, 1100, 2927, 3141 and 1530 cm^{-1} can be ascribed to the stretching vibrations of Si–O, C-N, C_{sp3}–H, C_{sp2}–H and C=C and confirmed the surface functionalization of the MNPs. The FT-IR spectra of γ-Fe_2O_3-Im-butyl-SO_3Na and γ-Fe_2O_3-Pd-NHC-*n*-butyl-SO_3Na display a typical band at around 1040 cm^{-1} corresponded to S=O stretching vibrations (Figure 1).

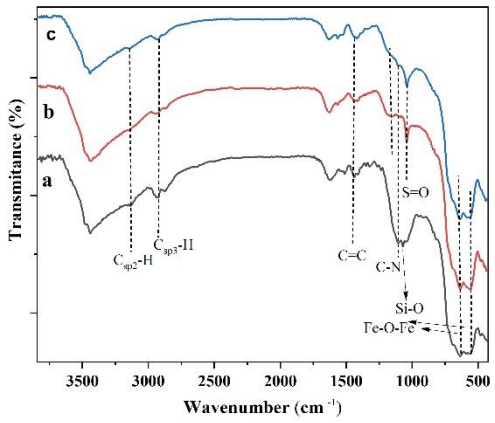

Figure 1. FT-IR spectra of (a) γ-Fe_2O_3-Im, (b) γ-Fe_2O_3-Im-*n*-butyl-SO_3Na and (c) γ-Fe_2O_3-Pd-NHC-*n*-butyl-SO_3Na

XPS study was performed to determine the presence of the elements in the sample and also the electronic properties of the atoms (Figure 2). In the XPS elemental survey of γ-Fe_2O_3-Pd-NHC-*n*-butyl-SO_3Na, the peaks corresponding to oxygen, carbon, nitrogen, silicon, iron, sodium, sulfur and palladium are clearly observed (Figure 2a). The C1s spectra could be fitted to three peaks with binding energies at 284.5 (C-C and C=C), 286.1 (C_{sp2}-N) and 288 eV (C_{sp3}-N) (Figure 2b).[63] The nitrogen region revealed the presence of a main peak at 401.3 eV related to C-N-C and 399.9 eV related to C_{sp3}-N (Figure 2c).[64] According to Figure 2d, the S2p spectrum mainly consisted of four peaks centred at 163.2, 164.2, 167.6 and 168.8 eV. The former two peaks could be attributed to $2p_{3/2}$ and $2p_{1/2}$ of the C–S bond and the latter two peaks could be related to $2p_{3/2}$ and $2p_{1/2}$ of the –SO_3Na species.[65] The peaks appeared at 337.8 ($3d_{5/2}$) and 342.9 eV ($3d_{3/2}$), are ascribed to Pd (II) (Figure 2e). A small portion of Pd (0) was also detected by the peaks at 335.4 ($3d_{5/2}$) and 340.5 eV ($3d_{3/2}$).[66]

ARTICLE

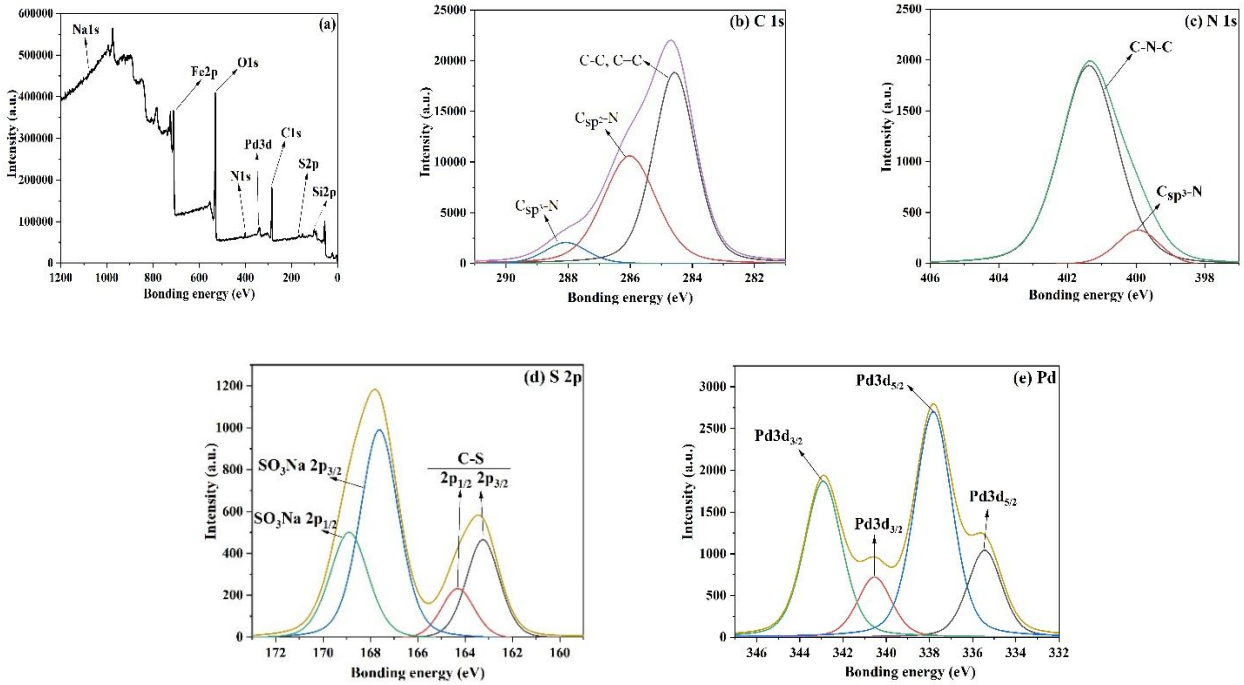

Figure 2. (a) XPS patterns of γ-Fe_2O_3-Pd-NHC-*n*-butyl-SO_3Na (b) C1s (c) N1s (d) S2p and (e) Pd.

The Pd loading of γ-Fe_2O_3-Pd-NHC-*n*-butyl-SO_3Na was measured by ICP. The ICP analysis showed that 0.21 mmol of Pd was anchored onto 1 g of γ-Fe_2O_3-Pd-NHC-*n*-butyl-SO_3Na.

The morphologies and sizes of the catalyst were investigated using transmission electron microscopy (TEM, Figure 3) and field emission scanning electron microscopy (FESEM, Figure 4). These images showed that γ-Fe_2O_3-Pd-NHC-*n*-butyl-SO_3Na NPs are spherical in shape. From the particle size histogram in Figure 3d, the nanoparticle size is about 9–15 nm with an average diameter of 12 nm. By comparison of the TEM images of γ-Fe_2O_3-Pd-NHC-*n*-butyl-SO_3Na (Figure 3a and 3b) with those of γ-Fe_2O_3 (Figure 3c), it is seen that γ-Fe_2O_3 modified by hydrophilic Pd-NHC could be highly dispersed in water. The chemical composition of γ-Fe_2O_3-Pd-NHC-*n*-butyl-SO_3Na was determined by EDX analysis. The peaks of Pd, C, N, S, O, Fe and Na confirmed the chemical modification of the nanocatalyst. Elemental mapping of γ-Fe_2O_3-Pd-NHC-*n*-butyl-SO_3Na was carried out to understand the distribution of elements in the catalyst as shown in Figure 4. From elemental mapping data, it is clear that all the elements are distributed evenly.

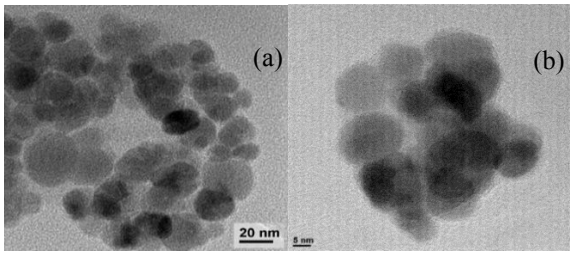

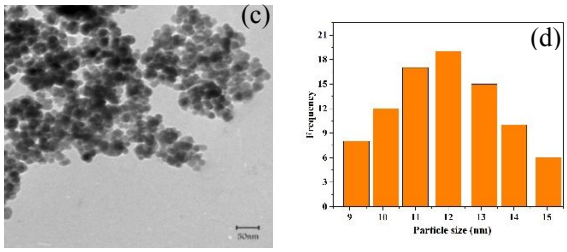

Figure 3. (a, b, c) TEM, (d) particle size distribution histogram of γ-Fe_2O_3-Pd-NHC-*n*-butyl-SO_3Na

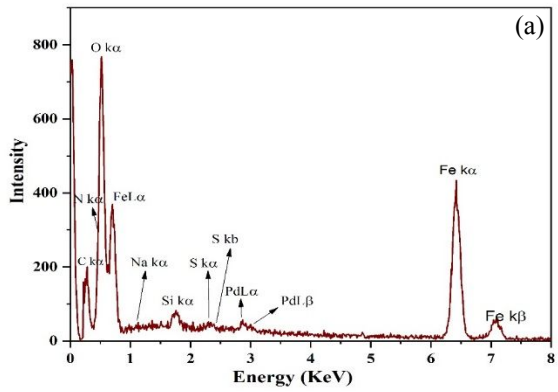

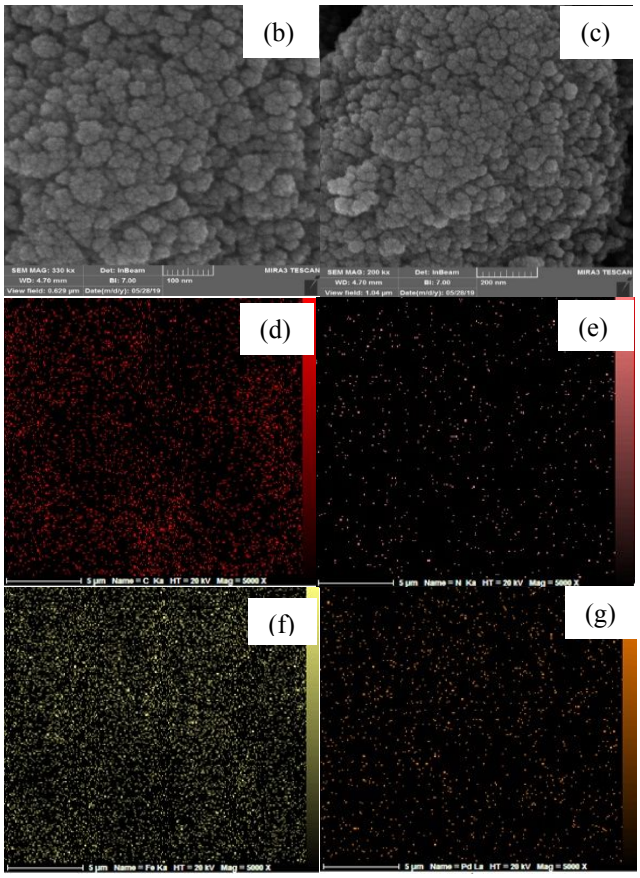

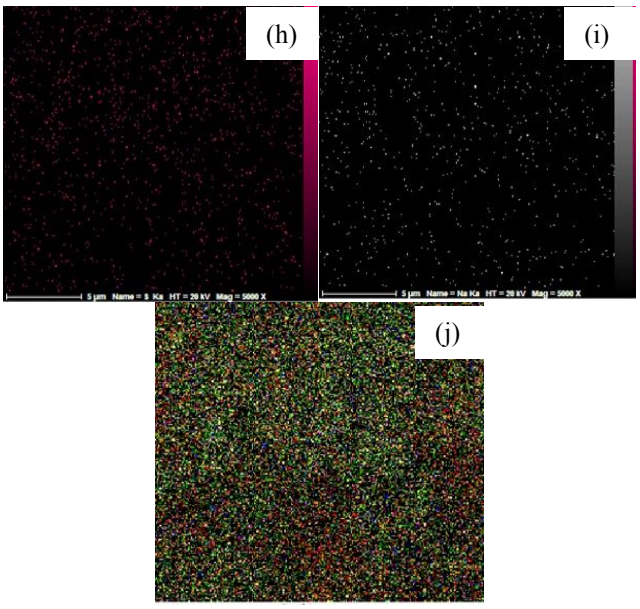

Figure 4. (a) EDX spectrum, (b, c) FESEM images of γ-Fe_2O_3-Pd-NHC-*n*-butyl-SO_3Na, and the corresponding quantitative EDS element mapping of (d) C, (e) N, (f) Fe, (g) Pd, (h) S, (i) Na and (j) all elements

The magnetic properties of the samples containing a magnetite component were studied by a vibrating sample magnetometer (VSM) at 300 ˚K (Figure 5). It shows the absence of hysteresis phenomenon and indicates that γ-Fe_2O_3-Pd-NHC-*n*-butyl-SO_3Na has superparamagnetic at room temperature. The saturation magnetization values for γ-Fe_2O_3 and γ-Fe_2O_3-Pd-NHC-*n*-butyl-SO_3Na were 68.5 and 65.9 emu/g, respectively. Small decrease in the saturated magnetization value of γ-Fe_2O_3-Pd-NHC-*n*-butyl-SO_3Na compared to that of γ-Fe_2O_3 can be attributed to the slight increase in mass owing to the immobilized Pd-complex on the surface of γ-Fe_2O_3. With this low reduction in the magnetization, the catalyst can still be separated easily from the solution by an external magnetic field.

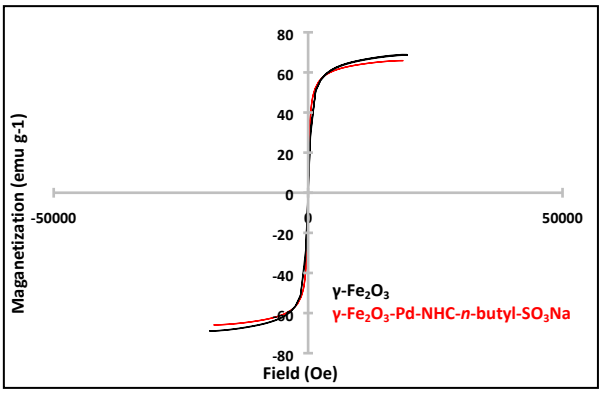

Figure 5. Magnetization curves of γ-Fe_2O_3(black) and γ-Fe_2O_3-Pd-NHC-*n*-butyl-SO_3Na (red)

The thermogravimetric analysis (TGA) was used to determine the thermal stability of γ-Fe_2O_3-Pd-NHC-*n*-butyl-SO_3Na. The weight loss below 168 °C is related to the adsorbed water molecules on the catalyst. The second weight loss of about 3% between 168 and 488 °C is attributed to the decomposition of organic components attached to the surface (Figure 6).

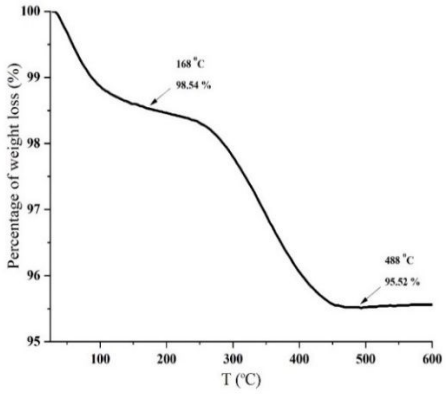

Figure 6. TGA diagram of γ-Fe_2O_3-Pd-NHC-*n*-butyl-SO_3Na

Hiyama, Suzuki and cyanation reactions catalyzed by γ-Fe_2O_3-Pd-NHC-*n*-butyl-SO_3Na in aqueous media

At first, in order to optimize the reaction conditions of Hiyama cross-coupling reaction, the coupling reaction of iodobenzene (1 mmol), triethoxyphenylsilane (1.2 mmol) and NaOH in the presence of γ-Fe_2O_3-Pd-NHC-*n*-butyl-SO_3Na (0.1 mol%) was chosen as a model reaction in aqueous media. The results of these studies are depicted in Figure 7. The coupling reaction was found to be sensitive to the reaction temperature. The highest yield was obtained at 80 °C (Figure 7a). The model reaction was studied in the presence of different amounts of the catalyst (Figure 7b). When 0.08 mol% of the catalyst was used, the best result was obtained. The effect of some bases such as NEt_3, KOH, NaOH, Na_2CO_3 and K_2CO_3 on the progress of the reaction was also investigated. Among the bases used, NaOH was found to be the most efficient base (Figure 7c). To reveal the effect of the hydrophobic group of the catalyst in the progress of the reaction, the model reaction in the presence of γ-Fe_2O_3-Pd-NHC-Me (Scheme 2) was investigated. The reaction proceeds to produce 31% of the corresponding biaryl in 4 h and remained constant even after 24 h (Figure 7b). These results demonstrate that γ-Fe_2O_3-Pd-NHC-*n*-butyl-SO_3Na in water is more active than γ-Fe_2O_3-Pd-NHC-*n*-Me, due to the presence of hydrophilic functional group, which provides a desirable dispersion of the catalyst in aqueous media (Figure 8).

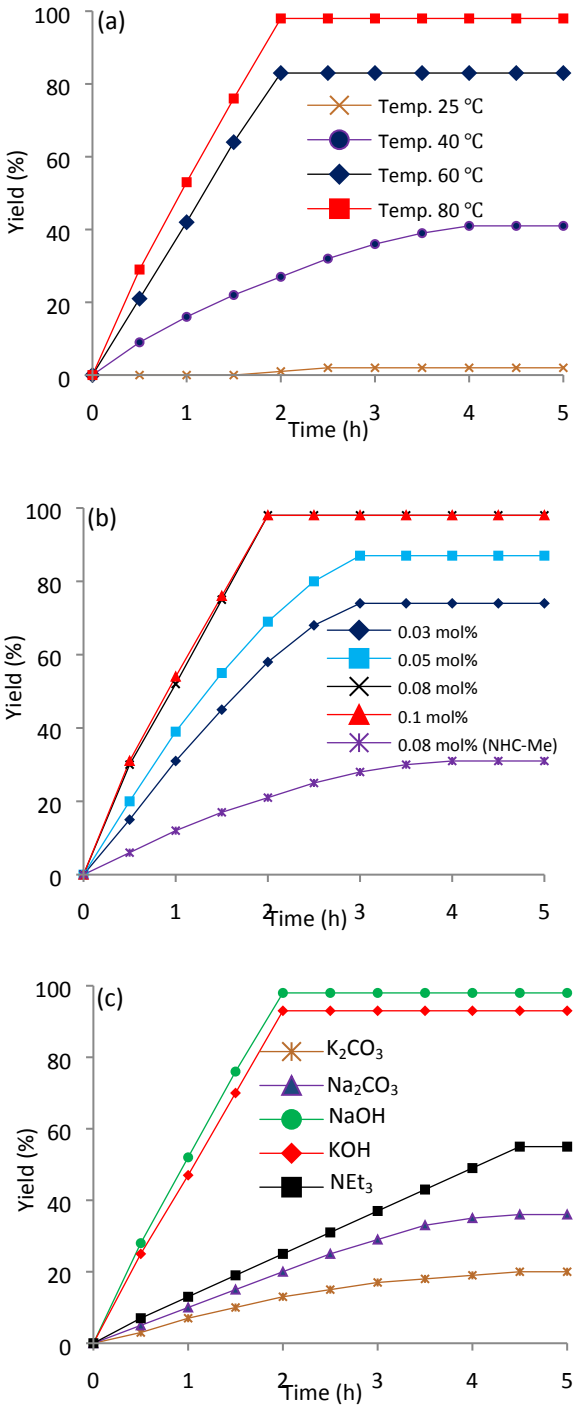

Figure 7. Optimizing reaction conditions such as (a) temperature, (b) amount of the catalyst and (c) base for the Hiyama cross-coupling reaction of iodobenzene with triethoxyphenylsilane catalyzed by γ-Fe_2O_3-Pd-NHC-*n*-butyl-SO_3Na in aqueous media

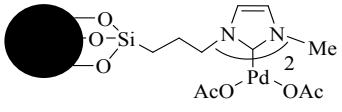

γ-Fe_2O_3-Pd-NHC-Me

Scheme 2. γ-Fe_2O_3-Pd-NHC-Me

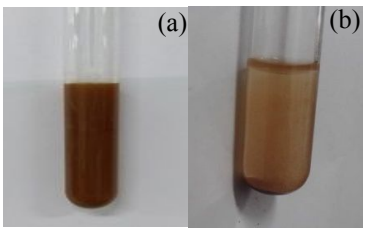

Figure 8. (a) γ-Fe_2O_3-Pd-NHC-*n*-butyl-SO_3Na in water and (b) γ-Fe_2O_3-Pd-NHC-Me in water

With the optimized reaction conditions in hand, the substrate scope and limitation of the Hiyama cross-coupling reaction, were studied for the reaction of different aryl halides with triethoxyphenylsilane (Table 1). As shown in Table 1, the cross-coupling reaction of various aryliodides, bromides and chlorides (cheaper and more widely available than aryl iodides and bromides) containing electron-withdrawing and electron-releasing groups with triethoxyphenylsilane proceeded well and the desired products produced in good to high yields without requiring any fluoride ion. Moreover, 1-chloro-4-iodobenzene and 1-bromo-4-chloro benzene chemoselectively furnished 4-chloro-biphenyl as the only product in 96 and 94% yields, respectively (Table 1, entries 3 and 7). It is worth to mention that in these reactions, any homo-coupling products were not obtained.

Table 1. Hiyama cross-coupling reaction of various aryl halides with triethoxyphenylsilane catalyzed by γ-Fe_2O_3-Pd-NHC-*n*-butyl-SO_3Na in aqueous media

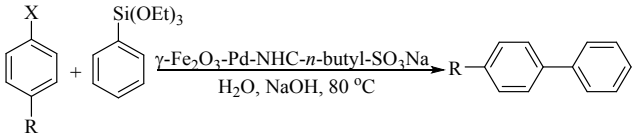

Entry	X	R	Product	Time (h)	Isolated yields[a] (%)
1	I	H	**1**	2	98
2	I	OMe	**2**	4	92
3	I	Cl	**3**	2.5	96
4	I	I	**4**	9	86
5	Br	H	**1**	2.5	95
6	Br	OMe	**2**	4.5	90
7	Br	Cl	**3**	3	94
8	Br	CN	**5**	4.5	92
9	Cl	H	**1**	4	93
10	Cl	NO_2	**6**	7	80[b]
11	Cl	CN	**5**	6	90

[a] Isolated yields. Reaction conditions: aryl halide (1 mmol), phenyltriethoxysilane (1.2 mmol), NaOH (2 mmol), H_2O (4 mL), catalyst (0.08 mol%, except for entry 10). [b] Catalyst (0.16 mol%).

Promising results obtained from Hiyama reaction, induced us to evaluate the catalytic activity of γ-Fe_2O_3-Pd-NHC-*n*-butyl-SO_3Na in the Suzuki cross-coupling reaction of halobenzenes with phenylboronic acid in aqueous media. For this purpose, the reaction of iodobenzene (1 mmol), phenylboronic acid (1.2 mmol) and K_2CO_3 in the presence of γ-Fe_2O_3-Pd-NHC-*n*-butyl-SO_3Na (0.1 mol%) in aqueous media was selected as a benchmark reaction to optimize the reaction parameters such as the amount of the catalyst and kind of the base (Figure 9). As the temperature plays an important role in promoting Suzuki reactions, we have chosen ambient temperature as the reaction temperature. The model reaction was studied in the presence of different amounts of the catalyst (Figure 9a). The best result was obtained in the presence of 0.08 and 0.1 mol% of the catalyst. We have chosen the lower amount of the catalyst (0.08 mol%) for the rest of the reactions. To investigate the effect of the base in this transformation, model reaction was carried out in the presence of Na_2CO_3, NaOH, KOH and NEt_3 (Figure 9b). It was found that the reaction proceeded with lower product yields and over prolonged reaction times in the presence of these bases compared with K_2CO_3 (Figure 9b).

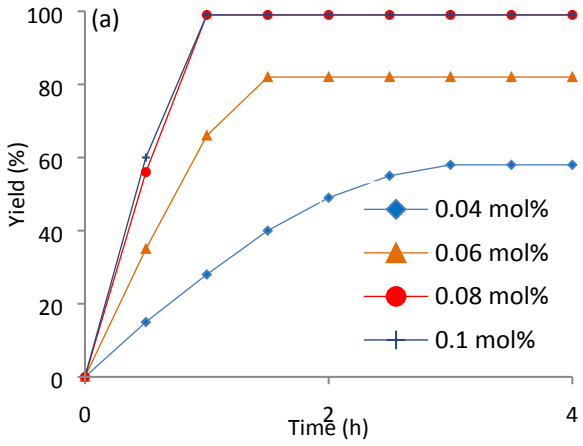

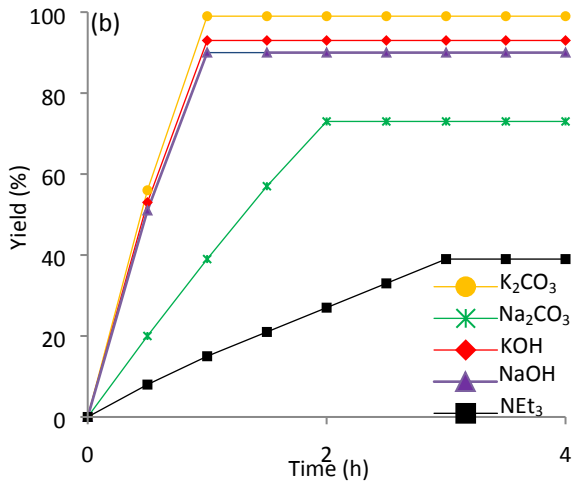

Figure 9. Optimizing reaction conditions such as (a) amount of the catalyst and (b) base for the Suzuki-Miyaura cross-coupling reaction of iodobenzene with phenylboronic acid catalyzed by γ-Fe_2O_3-Pd-NHC-*n*-butyl-SO_3Na in aqueous media at room temperature.

To investigate the scope and generality of the Suzuki–Miyaura cross-coupling reaction, we have studied the reaction of a range of aryl halides with phenylboronic acid under the aforementioned optimized reaction conditions and the results are summarized in Table 2. All the aryl iodides and bromides with electron-withdrawing or electron-releasing groups reacted with phenylboronic acid to afford the corresponding products in high yields (Table 2, entries 1-8). Importantly, aryl chlorides which have stronger carbon halogen bond, underwent the coupling reaction and gave the desired products in high yields (Table 2, entries 9-11). Additionally, γ-Fe_2O_3-Pd-NHC-*n*-butyl-SO_3Na was further studied towards the selectivity through conducting the Suzuki–Miyaura cross-coupling reactions using the optimized reaction conditions in the absence of phenylboronic acid. The biphenyl homo-coupled products was not formed even after 24 h. Hence, it is concluded that our newly synthesized catalyst is highly selective.

Table 2. Suzuki–Miyaura cross-coupling reactions of various aryl halides and phenylboronic acid catalyzed by γ-Fe_2O_3-Pd-NHC-*n*-butyl-SO_3Na in aqueous media

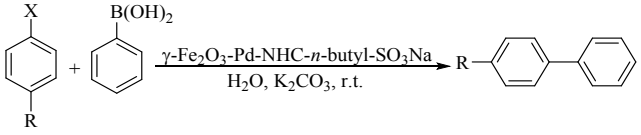

Entry	X	R	Product	Time (h)	Isolated yields[a] (%)
1	I	H	**1**	1	99
2	I	OMe	**2**	9	94
3	I	Cl	**3**	8	97
4	I	I	**4**	6	82
5	Br	H	**1**	2	97
6	Br	OMe	**2**	15	91
7	Br	Cl	**3**	9	95
8	Br	CN	**5**	6.5	92
9	Cl	H	**1**	5	95[b]
10	Cl	NO_2	**6**	13	82[b]
11	Cl	CN	**5**	11	85[b]

[a] Isolated yields. Reaction conditions: aryl halide (1 mmol), phenylboronic acid (1.2 mmol), K_2CO_3 (2 mmol), H_2O (4 mL), catalyst (0.08 mol%, except for entries 9-11). [b] Catalyst (0.16 mol%).

Encouraged by the results obtained during the Hiyama and Suzuki reactions catalyzed by γ-Fe_2O_3-Pd-NHC-*n*-butyl-SO_3Na in water, we investigated the catalytic reactivity of γ-Fe_2O_3-Pd-NHC-*n*-butyl-SO_3Na in the cyanation reaction. In this regards, the reaction of iodobenzene (1 mmol, $K_4[Fe(CN)_6]\cdot 3H_2O$ (1.2 mmol) and NEt_3 in the presence of γ-Fe_2O_3-Pd-NHC-*n*-butyl-SO_3Na (0.3 mol%) in aqueous media was selected at 90 °C to optimize the reaction conditions. Based on the results indicated in Figure 10, $K_4[Fe(CN)_6]\cdot 3H_2O$, Et_3N, 90 °C and 0.2 mol% of the catalyst were chosen as the best conditions (Figure 10).

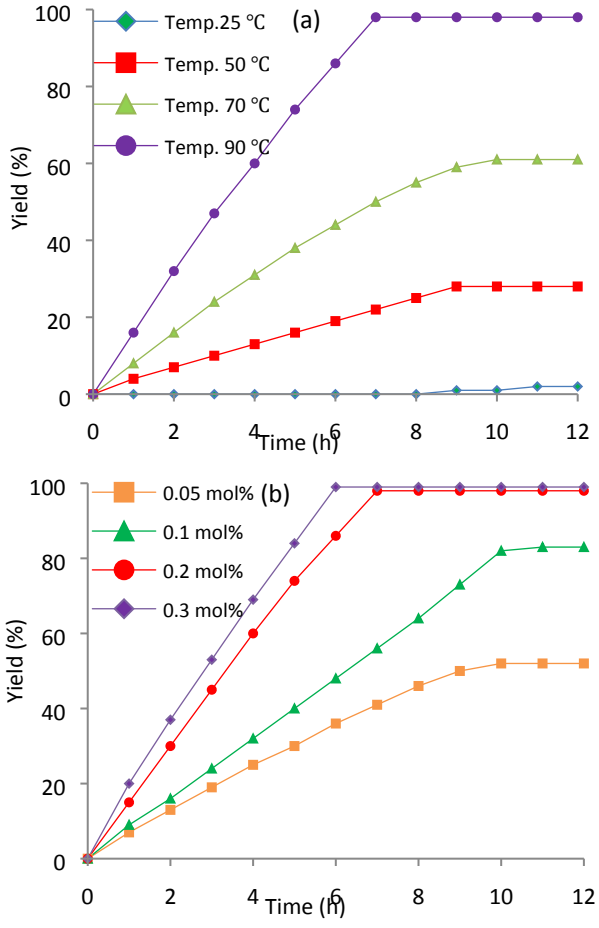

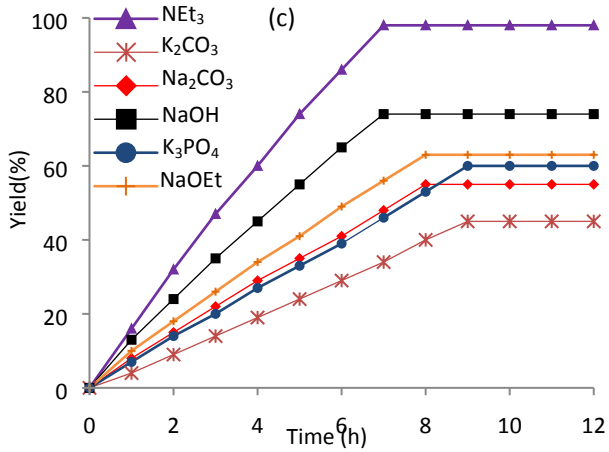

Figure 10. Optimizing reaction conditions such as (a) temperature, (b) amount of catalyst and (c) base in the cyanation reaction of iodobenzene with $K_4[Fe(CN)_6]\cdot 3H_2O$ catalyzed by γ-Fe_2O_3-Pd-NHC-*n*-butyl-SO_3Na in aqueous media

To further investigate the scope and limitations of this protocol, various types of aryl halides were selected and allowed to react using the optimized reaction parameters (Table 3). Different aryl iodides, bromides and chlorides underwent the cyanation reaction and produced the desired aryl nitriles in good to high yields. This method was also applicable for the cyanation of aryl tosylate (Table 3, entry 18). It is worth to mention that 4-flourocyanobenzene was achieved by the selective replacement of bromine in 1-boromo-4-flourobenzene with $K_4[Fe(CN)_6]\cdot 3H_2O$ (Table 3, entry 10). Under the present reaction conditions, the coupling reaction of 1,4-diiodobenzene with $K_4[Fe(CN)_6]\cdot 3H_2O$ worked well to afford 4-iodocyanobenzene in 70% yields (Table 3, entry 3). Both halogens in 1,4-diiodo and 1,4-dibromobenzene were replaced by twice amounts of $K_4[Fe(CN)_6]\cdot 3H_2O$ under the present reaction conditions (Table 3, entries 4 and 11). 3-Bromopyridine also underwent the cyanation reaction and produced 3-cyanopyridine in 87% yields (Scheme 3).

Table 3. Cyanation of aryl halides with $K_4[Fe(CN)_6]\cdot 3H_2O$ in the presence of γ-Fe_2O_3-Pd-NHC-*n*-butyl-SO_3Na in aqueous media.

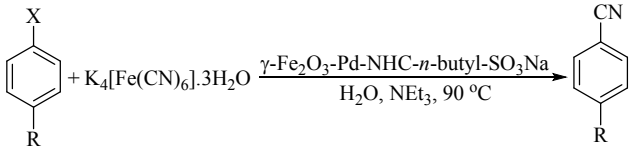

Entry	X	R	Product	Time (h)	Isolated yields[a] (%)
1	I	H	**7**	7	98
2	I	OMe	**8**	12	94
3	I	I	**9**	10	70
4	I	I	**10**	13	84[b]
5	Br	H	**7**	8	96
6	Br	Me	**11**	14	87
7	Br	OMe	**8**	13	89
8	Br	CN	**10**	12	91
9	Br	NO_2	**12**	15	87
10	Br	F	**13**	13	93
11	Br	Br	**10**	16	73[b]
12	Br	CHO	**14**	17	69
13	Cl	H	**7**	12	92[c]
14	Cl	Me	**11**	15	82[c]
15	Cl	NO_2	**12**	16	79[c]
16	Cl	CN	**10**	14	85[c]
17	Cl	CHO	**14**	24	56[c]
18	OTs	H	**7**	15	71[c]

[a] Isolated yields. Reaction conditions: aryl halide (1 mmol), $K_4[Fe(CN)_6]\cdot 3H_2O$ (1.2 mmol), Et_3N (4 mmol), H_2O (6 mL), catalyst (0.2 mol%, except for entries 13-18). [b]Reaction conditions: aryl halide (1 mmol), $K_4[Fe(CN)_6]\cdot 3H_2O$ (2.4 mmol), Et_3N (8 mmol), H_2O (6 mL), catalyst (0.2 mol%). [c]Catalyst (0.3 mol%).

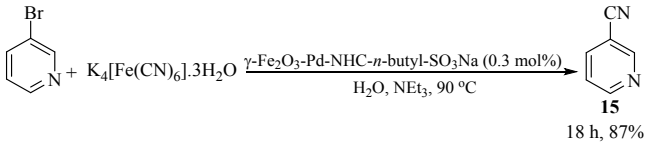

Scheme 3. Cyanation reaction of 3-bromopyridine

The resulted coupling products in the present study have widespread usages as vital building blocks in the preparation of numerous structurally different molecules in many areas of chemistry such as pharmaceuticals, material sciences, and agrochemicals. Biaryl functionalities are present in a wide range of therapeutic classes, including antifungal, antiinflammatory, antirheumatic, antitumor, and antihypertensive agents.[32,33] For instance, biaryl segment is the core structure of a number of drugs such as diflunisal (antipyretic non-steroidal anti-inflammatory), felbinac (anti-inflammatory) and fenbufen 3 (non-steroidal anti-inflammatory) (Scheme 4).[30,67,68] Several synthetic protocols have been introduced for the construction of functionalized biaryls,[69,70] with most of them relying on the C–C cross-coupling reactions. One of the greatest common processes includes the metal-catalyzed Hiyama and Suzuki coupling reactions.[71,72] So, by considering the performing importance of large-scale reactions, in the next experiment we have evaluated the scalability of the Hiyama and Suzuki reactions. In this regard, the reactions of iodobenzene (50 mmol) and triethoxyphenylsilane (60 mmol) or phenylboronic acid (60 mmol) were performed under the present reaction conditions. The reactions proceeded in 2 and 1 h, and the desired products were obtained in 97 and 98% yields in Hiyama and Suzuki–Miyaura cross-coupling reactions, respectively. Benzonitriles represent an integral part of dyes, herbicides, agrochemicals, pharmaceuticals, and natural products.[45-47] Some examples of benzonitriles and

their main properties are presented in Scheme 4.[73] Moreover, the nitrile groups serve as intermediates for a multitude of transformations into other important functional groups.[74]

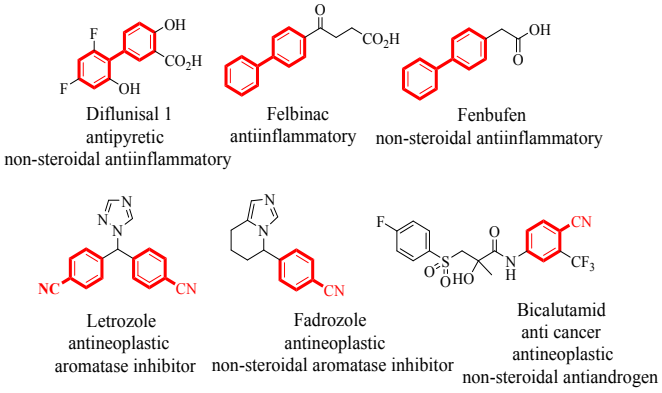

Scheme 4. Some examples of compounds containing biaryls and aryl nitriles with biological activity

From both practical and environmental points of view, the recovery and recycling of supported catalysts are very important issues. Along this line, the reusability of the catalyst was investigated in the model reaction of iodobenzene in Hiyama, Suzuki–Miyaura and cyanation reactions with triethoxyphenylsilane, phenylboronic acid and $K_4[Fe(CN)_6]\cdot 3H_2O$, respectively, under optimized reaction conditions. Considering the hydrophilic property of γ-Fe_2O_3-Pd-NHC-*n*-butyl-SO_3Na, after the first use of the catalyst, the product was simply extracted by EtOAc, while the catalyst remained in the aqueous phase (Figure 11b). Without any isolation of the catalyst, the aqueous phase was recharged with iodobenzene, the coupling partner {triethoxyphenylsilane, phenylboronic acid, $K_4[Fe(CN)_6]\cdot 3H_2O$} and the base for the next run. As shown in Figure 12, the catalyst could be reused for seven consecutive runs without any significant loss of its activity. To end, the catalyst was separated from the aqueous phase using an external magnetic field (Figure 11d).

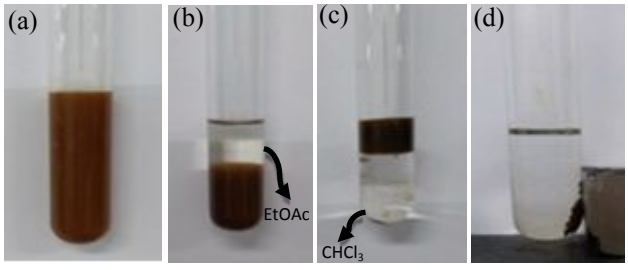

Figure 11. Dispersion of γ-Fe_2O_3-Pd-NHC-*n*-butyl-SO_3Na in water (a), distribution of γ-Fe_2O_3-Pd-NHC-*n*-butyl-SO_3Na in a biphasic water/EtOAc (b), distribution of γ-Fe_2O_3-Pd-NHC-*n*-butyl-SO_3Na in a biphasic water/ $CHCl_3$ system (c), and easy separation of γ-Fe_2O_3-Pd-NHC-*n*-butyl-SO_3Na using an external magnet (d)

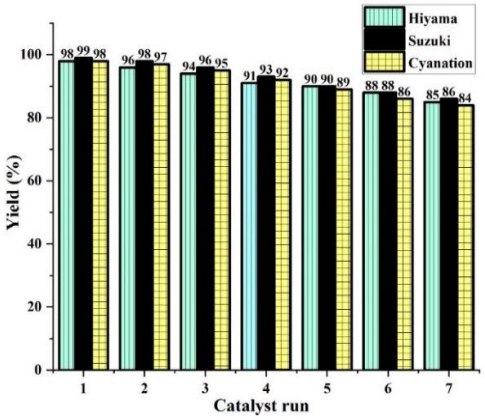

Figure 12. Reusability of γ-Fe_2O_3-Pd-NHC-*n*-butyl-SO_3Na in the model reactions of Hiyama (2 h), Suzuki–Miyaura (1 h) and cyanation (7 h) reactions

FT-IR spectrum, XPS pattern and TEM image of the recycled catalyst in the model Hiyama cross-coupling reaction after seven runs were investigated (Figure 13a-c). This study exhibited that the morphology and structure of the catalyst remained intact even after seven recoveries. Moreover, it can be clearly perceived from the dispersion of the catalyst in the aqueous media that the hydrophilic characteristic of the catalyst remained intact (Figure 13d).

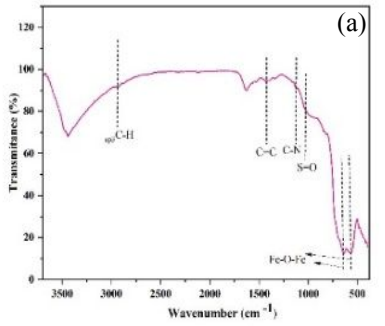

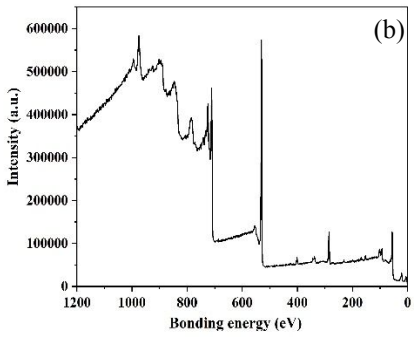

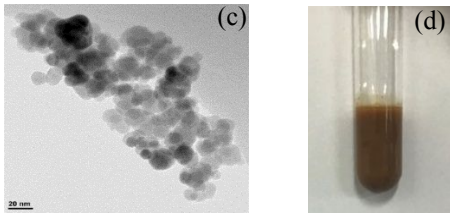

Figure 13. (a) FT-IR spectrum (b) XPS pattern, (C) TEM image and (d) dispersion of γ-Fe_2O_3-Pd-NHC-*n*-butyl-SO_3Na after seven catalyst recoveries in the model Hiyama cross-coupling reaction.

In addition, the recycled catalyst was also studied by ICP analysis to measure metal leaching. The leaching was very low, so that after the 7th recovery, the leaching amount was less than 0.1%, that was negligible. The presence of NHC moiety in the catalyst backbone prevented metal leaching in the aqueous media, which remains catalytic activity for practical goals due to its water stability.

In order to find out if the active catalyst is truly acting as a heterogeneous catalyst, hot filtration and poisoning tests were carried out for the Hiyama model reaction. In the hot filtration test, after completion of 50% of the reaction, the catalyst was isolated at the reaction temperature and the liquid phase was permitted to react for 24 h. Further conversion was not observed. This observation showed that any homogeneous catalyst was not present in the reaction mixture. In the poisoning test, the model reaction was evaluated in the presence and in the absence of S_8 (0.05 g) at 80 °C. The results are illustrated in Figure 14. As it is apparent, the presence of scavenger has no effect on the reaction progress and the desired product was obtained in excellent yield after 2 hours. The results of these two tests clearly demonstrated the true heterogeneous nature of the catalyst.

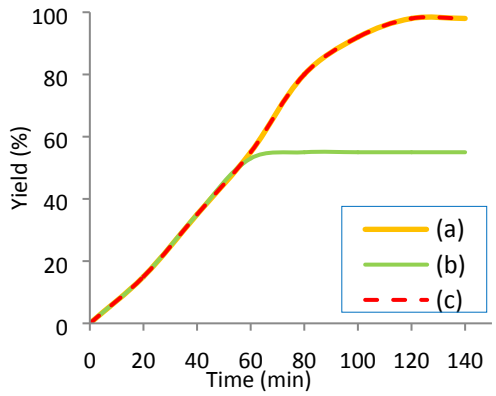

Figure 14. (a) Hiyama cross-coupling reaction of iodobenzene with triethoxyphenylsilane catalyzed by γ-Fe_2O_3-Pd-NHC-*n*-butyl-SO_3Na, (b) hot filtration test, (c) poisoning test using S_8

On the basis of the reported mechanism in the literature[75-77], a plausible mechanism for the catalytic cycle of Hiyama, Suzuki and cyanation reactions are proposed in Scheme 5. The mechanism begins with the preactivation of Pd(II) species of γ-Fe_2O_3-Pd-NHC-*n*-butyl-SO_3Na to Pd(0). Initially, oxidative addition of the aryl halide to the NHC-Pd(0) (**A**) was occurred to form an aryl-Pd(II) complex (**B**). Then, transmetallation of **B** with triethoxyphenylsilane, phenylboronic acid or potassium hexacyanoferrate (II) trihydrate $\{K_4[Fe(CN)_6]\cdot 3H_2O\}$ in the Hiyama, Suzuki and cyanation reactions, respectively, formed adduct **C**. Finally, reductive elimination gives the products (biaryl or aryl nitriles), and regenerates the palladium catalyst to repeat the catalytic cycle. In order to check a possible radical mechanism for the Hiyama coupling reaction, the reaction of iodobenzene with triethoxyphenylsilane was examined under the optimized reaction conditions in the presence of an electron trap such as hydroquinone. Hydroquinone was added to the reaction mixture after 1 h. No considerable changes were observed in the progress of the reaction. This result showed that no radicals were formed during the coupling process (Figure 15).

In addition, in order to investigate the mechanism more precisely, XPS analysis was performed *in situ* for the model Hiyama reaction. In the high resolution XPS spectrum of the Pd 3d of the catalyst (removed after 1 h of the reaction) (Figure 16), four main peaks located at 342.6, 337.5 eV and 340.4, 335.2 eV were observed, which confirmed the presence of both Pd(II) and Pd(0) species during the catalytic cycle. The amount of Pd(0) is more than Pd(II). These results supported the reduction of Pd(II) to Pd(0) (catalyst pre-activation) under the experimental conditions.

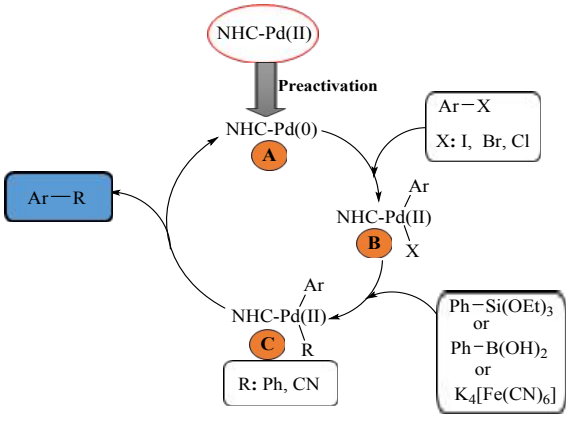

Scheme 5. Proposed mechanism of the Hiyama, Suzuki and cyanation reactions

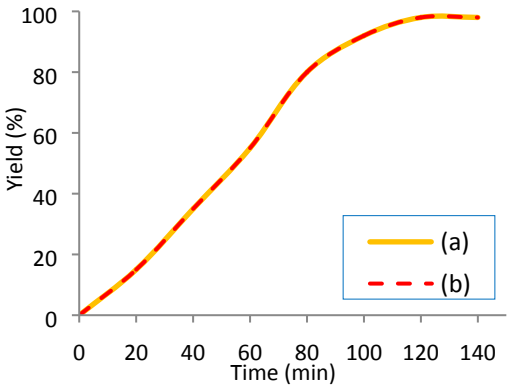

Figure 15. Hiyama cross-coupling reaction of idodobenzene with triethoxyphenylsilane catalyzed by γ-Fe_2O_3-Pd-NHC-*n*-butyl-SO_3Na in aqueous media (a) under normal reaction conditions and (b) in the presence of an electron trap.

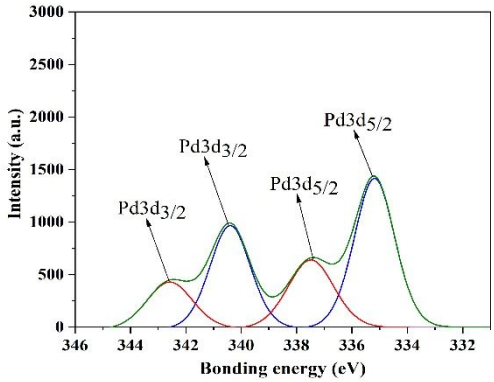

Figure 16. XPS pattern of Pd 3d after 1 h in the model Hiyama reaction

To show the merit of the current protocol for the synthesis of biaryls and arylnitriles, we have compared our results obtained for Hiyama, Suzuki and cyanation reactions with some of those reported in the literature using heterogeneous catalysts in aqueous media (Table 4). Among the heterogeneous catalysts in Table 4, the present catalytic system, exhibited higher catalytic activity in terms of turnover number (TON) with lower amount of the catalyst and at lower temperatures, in pure water as reaction media without using any additives and co-solvent. Moreover, most aryl halides were not competent substrates with the reported systems. The obtained results in the presence of γ-Fe_2O_3-Pd-NHC-*n*-butyl-SO_3Na should be related to the water dispersibility of the catalyst. The water-dispersibility makes the better contact between the catalyst and the reactants, thus increasing the catalytic activity and stability of the catalyst. It is important to note that our catalyst is the first heterogeneous NHC-Pd catalyst for the cyanation of aryl halides in aqueous media.

Table 4. Comparison of efficiency of various heterogeneous palladium catalysts in Hiyama, Suzuki-Miyaura and cyanation reactions with γ-Fe_2O_3-Pd-NHC-*n*-butyl-SO_3Na in aqueous media

Entry	Reactions	Catalyst (mol%)	Reaction conditions	Aryl halides	Isolated yields (%)	Time (h)	TON[a]
1[78]	Hiyama cross-coupling	IL@SBA-15-NHC-Pd (0.8)	TBAF, Cs_2CO_3, Dioxane: H_2O, 80 ˚C	I	94-95	8	117.5-118
				Br	82-93	5-8	102.5-112
2[79]	Hiyama cross-coupling	Fe_3O_4@SiO_2/ APTMS[b]/Pd(cdha[c])$_2$ (0.22)	NaOH, SDS, H_2O, 100 ˚C	I	100	5 min	454
				Br	63-100	5 min	286-454
				Cl	68-82	5 min	309-372
3[80]	Hiyama cross-coupling	Pd/Fe_3O_4 (1)	NaOH, H_2O, 90 ˚C	Br	0-96	3-4	0-455
4[81]	Hiyama cross-coupling	Pd@DCA[d]-MCM nanocomposite (0.1)	NaOH, H_2O: EtOH, 80 ˚C	I	88-91	3	880-910
				Br	85-90	3	850-900
5[82]	Hiyama cross-coupling	PS-PdONPs (1.5)	NaOH, H_2O, TBAC[e], 80 ˚C	Br	10-88	3	6.6-58.6
6[This work]	Hiyama cross-coupling	γ-Fe_2O_3- Pd-NHC-*n*-butyl-SO_3Na (0.08, 0.16)	NaOH, H_2O, 80 ˚C	I	86-98	2-9	1075-1212
				Br	90-95	2.5-4.5	1037-1187
				Cl	80-93	4-7	500-1162
7[83]	Suzuki-Miyaura reaction	Fe_3O_4@SiO_2-NHC-Pd (0.37, 0.5)	K_2CO_3, H_2O, 60 ˚C	I	90-97	1-2.5	243-262
				Br	87-96	2-4	235-259
				Cl	69-83	12-20	138-166
8[84]	Suzuki-Miyaura reaction	GO-NHC-Pd complex (0.1)	K_2CO_3, EtOH: H_2O (1: 1), TBAB, r.t.	Br	51-99	0.5-24	510-990
9[85]	Suzuki-Miyaura reaction	AP[f] Pd(0)@Si (1)	K_2CO_3, H_2O, 80 ˚C	Br	43-100	1-24	43-100

10[86]	Suzuki-Miyaura reaction	MNPs@SB[g]-Pd (0.15)	K_2CO_3, EtOH: H_2O (1: 1), r.t.	I	80	2	147
				Br	65-91	2-23	433-606
				Cl	37-60	12-15	246-400
11[87]	Suzuki-Miyaura reaction	GO–NHC–Pd (1)	Cs_2CO_3, DMF: H_2O, 50 ˚C	I	94-99	1	94-99
				Br	81-99	1	81-99
				Cl	28-37	1	28-37
12[88]	Suzuki-Miyaura reaction	NO_2-NHC-Pd@Fe_3O_4 (0.15)	K_2CO_3, EtOH:H_2O (1: 1), r.t.	I	90-96	1-4	600-640
				Br	85-96	2-12	566-640
				Cl	89	4	593.3
13[89]	Suzuki-Miyaura reaction	Pd(0/II)/CS-bigua[h]@Fe_3O_4 (0.2)	K_2CO_3, EtOH:H_2O (1: 1), r.t.	I	90-96	1-4	450-480
				Br	85-96	2-12	425-480
				Cl	30-40	24	150-200
14[90]	Suzuki-Miyaura reaction	Pd/CPP[i] (0.55)	$K_3PO_4.3H_2O$, EtOH:H_2O (3: 2), r.t.	Br	93-99	1-2	169-180
				Cl	82-98	5	149-170
15[This work]	Suzuki-Miyaura reaction	γ-Fe_2O_3- Pd-NHC-*n*-butyl-SO_3Na (0.08, 0.16)	K_2CO_3, H_2O, r.t.	I	82-99	1-9	1025-1237
				Br	91-97	2-15	1137-1237
				Cl	82-95	5-13	512-594
16[91]	Cyanation	Pd-CD-PU-NS[j] (1.7)	Na_2CO_3, DMF:H_2O (1: 1), 120 ˚C	I	70	15	41
				Br	60	15	35
17[92]	Cyanation	Pd/C (10)	KI, NaF, H_2O:PEG 4000,MW/100–160 ˚C	I	60-97	2	6-9.7
				Br	70-95	2-3	7-9.5
				Cl	0-48	2	0-4.8
18[93]	Cyanation	$Pd(OAc)_2$ (5)	NaF: TBAB[k]: H_2O, 150 ˚C /MW	I	0-94	20 min	0-18.8
				OTs	43-96	18	21.5-48
19[94]	Cyanation	$Pd(dba)_2$[l] (2)	t-BuOH: H_2O, K_2CO_3, 80 ˚C	Cl	0-48	2	0-4.8
				OMs	67-95	18	33.5-48.5
20[This work]	Cyanation	γ-Fe_2O_3- Pd-NHC-*n*-butyl-SO_3Na (0.2, 0.3)	NEt_3, H_2O, 90 ˚C	I	70-98	7-13	350-490
				Br	69-96	8-18	345-480
				Cl	56-92	12-24	186-306
				OTs	71	15	236

[a]Turnover number (TON = mol of the product per mol of the catalyst).
[b]APTMS=3-aminopropyltrimethoxysilane.
[c]cdha=bis(2-chloro-3,4-dihydroxyacetophenone.
[d]DCA=1,2-dicarboxylic groups.
[e]TBAC= tetrabutylammonium chloride.
[f]AP= 3-aminopropyl.
[g]SB= Schiff-base.
[h]CS-bigua= Chitosan-biguanidine**.**
[i]CPP=conjugated phenanthroline based porous polymer.
[j]CD-PU-NS= Cyclodextrin-polyurethane nanosponge.
[k]TBAB=Tetrabutylammonium bromide.
[l]dba=dibenzylideneacetone.

Conclusion

In summary, a water-dispersible Pd-*N*-heterocyclic carbene complex immobilized on magnetic nanoparticles was synthesized and characterized by different techniques such as FT-IR, XPS, TEM, EDX, FESEM, VSM, TGA and ICP analysis. The synthesized catalyst was used as a new water dispersible heterogeneous catalyst in the fluoride-free Hiyama, Suzuki and cyanation reactions. By this method, different types of biaryls and aryl nitriles were synthesized in good to high yields by the reaction of a variety of aryl iodides, bromides and chlorides with triethoxyphenylsilane, phenylboronic acid and $K_4[Fe(CN)_6]\cdot 3H_2O$, respectively, in pure water without using any additives and co-solvent. The presence of sulfonates as hydrophilic groups on the surface of the catalyst generates a stable dispersion of the catalyst in water as the reaction medium and exposes the active palladium sites to substrates like homogeneous systems, thus increased the catalytic activity. The catalyst exhibited extremely low solubility in organic solvents. Using this property, the recovered aqueous phase containing the catalyst was simply and efficiently used in seven consecutive runs without a significant decrease in activity. At the end of the process the catalyst was easily isolated from the aqueous phase by using an external magnetic field. Hot filtration and poisoning tests indicated that the catalytic reaction was mainly heterogeneous in nature. The possibility to perform the reaction in water as a green medium, easy

catalyst recovery and reuse by successive extraction and final magnetic separation, and not requiring any additive or co-solvent make this method a valid candidate towards the goal of green chemistry for the synthesis of biaryl derivatives and aryl nitriles.

Supporting Information

This file contains general information of the NMR instrument, and ^{1}H NMR and ^{13}C NMR spectra of the products.

Acknowledgments

Financial support for this project from the University of Birjand Research Council is acknowledged. Access to the XPS facilities of the Central Technical Services of the University of Alicante is appreciated.

References

1. P. A. Grieco, *Springer*, Netherlands, 1998.
2. K. Kandhasamy and V. Gnanasambandam, *Curr. Org. Chem.*, 2009, **13**, 1820-11841.
3. E. Levin, E. Ivry, Charles E. Diesendruck and N. Gabriel Lemcoff, *Chem. Rev*., 2015, **115**, 4607-4692.
4. R. Breslow, *J. Am. Chem. Soc*., 1958, **80**, 3719-3726.
5. M. Poyatos, J. A. Mata and E. Peris, *Chem. Rev*., 2009, **109**, 3677-3707.
6. A. T. Normand and K. J. Cavell, *Eur. J. Inorg. Chem*., 2008, **2008**, 2781-2800.
7. O. Schuster, L. Yang, H. G. Raubenheimer and M. Albrecht, *Chem. Rev*., 2009, **109**, 3445-3478.
8. D. Enders, O. Niemeier and A. Henseler, *Chem. Rev*., 2007, **107**, 5606-5655.
9. S. Diez-Gonzalez, N. Marion and S. P. Nolan, *Chem. Rev*., 2009, **109**, 3612-3676.
10. P. de Fremont, N. Marion and S. P. Nolan, *Coord. Chem. Rev*., 2009, **253**, 862-892.
11. E. A. B. Kantchev, C. J. O'Brien and M. G. Organ, *Angew. Chem. Int. Ed.,* 2007, **46**, 2768-2813.
12. K. Arentsen, S. Caddick and F. G. N. Cloke, *Tetrahedron*, 2005, **61**, 9710-9715.
13. C. Boztepe, A. Künkül, S. Yaşar and N. Gürbüz, *J. Organomet. Chem*., 2018, **872**, 123-134.
14. G. C. Fortman and S. P. Nolan, *Chem. Soc. Rev*., 2011, **40**, 5151-5169.
15. N. T. S. Phan, D. H. Brown and P. Styring, *Tetrahedron Lett*., 2004, **45**, 7915-7919.
16. N. Gurbuz, I. Oezdemir, B. Cetinkaya and T. Seckin, *Appl. Organomet. Chem*., 2003, **17**, 776-780.
17. N. Shang, S. Gao, C. Feng, H. Zhang, C. Wang and Z. Wang, *RSC Adv*., 2013, **3**, 21863-21868.
18. M. Ghotbinejad, A. R. Khosropour, I. Mohammadpoor-Baltork, M. Moghadam, S. Tangestaninejad and V. Mirkhani, *J. Mol. Catal. A Chem*., 2014, **385**, 78-84.
19. S. Sobhani, Z. Pakdin-Parizi and R. Nasseri, *J. Chem. Sci.,* 2013, **125**, 975-979.
20. S. Sobhani, M. Bazrafshan, A. A. Delluei and Z. P. Parizi, *Appl. Catal. A Gen*., 2013, **454**, 145-151.
21. S. Sobhani and M. Honarmand, *Appl. Catal. A Gen*., 2013, **467**, 456-462.
22. A. J. Wagstaff, S. D. Brown, M. R. Holden, G. E. Craig, J. A. Plumb, R. E. Brown and N. J. Wheate, *Inorganica Chim. Acta*, 2012, **393**, 328-333.
23. N. Shahabadi, M. Falsafi, F. Feizi and R. Khodarahmi, *RSC Adv*., 2016, **6**, 73605-73616.
24. J. Liu, Z. Sun, Y. Deng, Y. Zou, C. Li, X. Guo and D. Zhao, *Angew. Chem. Int. Ed*., 2009, **48**, 5875-5879.
25. X. Liu, X. Zhao and M. Lu, *Appl. Organomet. Chem*., 2015, **29**, 419-424.
26. J. Afsar, M. A. Zolfigol and A. Khazaei, *ChemistrySelect*, 2018, **3**, 11134-11140.
27. H. Salemi, B. Kaboudin, F. Kazemi and T. Yokomatsu, *RSC Adv*., 2016, **6**, 52656-52664.
28. C. J. Li, *Chem. Rev*., 2005, **105**, 3095-3166**.**
29. V. H. Thorat, N. S. Upadhyay and C. H. Cheng, *Adv. Synth. Catal*., 2018, **360**, 4784-4789.
30. T. Kylmälä, J. Tois, Y. Xu and R. Franzén, *Open Chem*., 2009, **7**, 818-826.
31. S. Yuan, J. Chang and B. Yu, *Top. Curr. Chem*., 2020, **378**, 1-70.
32. K. Bahrami and H. Targhan, *Appl. Organomet. Chem*., 2019, **33**, e4842.
33. N. Miyaura, *J. Organomet. Chem*., 2002, **653**, 54-57.
34. A. J. J. Lennox and G. C. Lloyd-Jones, *Chem. Soc. Rev*., 2014, **43**, 412-443.
35. H. F. Sore, W. R. J. D. Galloway and D. R. Spring, *Chem. Soc. Rev*., 2012, **41**, 1845-1866.
36. T. Hiyama and Y. Hatanaka, *Pure Appl. Chem*., 1994, **66**, 1471-1478.
37. Y. Hatanaka and T. Hiyama, *Synlett*, 1991, **1991**, 845-853.
38. E. Alacid and C. Najera, *Adv. Synth. Catal*., 2006, **348**, 2085-2091.
39. C. Wolf and R. Lerebours, *Org. Lett*., 2004, **6**, 1147-1150.

40. M. Keller, V. Collière, O. Reiser, A. M. Caminade, J. P. Majoral and A. Ouali, *Angew. Chem. Int. Ed*., 2013, **52**, 3626-3629.
41. M. J. Jin and D. H. Lee, *Angew. Chem. Int. Ed*., 2010, **49**, 1119-1122.
42. S. Rostamnia, B. Zeynizadeh, E. Doustkhah and H. G. Hosseini, *J. Colloid Interface Sci*., 2015, **451**, 46-52.
43. L. Liu, Y. Zhang and Y. Wang, *J. Org. Chem*., 2005, **70**, 6122-6125.
44. A. Monfared, R. Mohammadi, S. Ahmadi, M. Nikpassand and A. Hosseinian, *RSC Adv*., 2019, **9**, 3185-3202.
45. J. Wang, H. Liu, W. Jiang and L. Hong, Chin. *J. Org. Chem*., 2012, **32**, 1643-1652.
46. F. F. Fleming, *Nat. Prod. Rep*., 1999, **16**, 597-606.
47. R. C. Larock, *Wiley-VCH: Weinheim*, Germany,1989, 819-995.
48. K. W. Rosenmund and E. Struck, *Eur. J. Inorg. Chem*., 1919, **52**, 1749-1756.
49. A. C. Stevenson, *Ind. Eng. Chem*., 1948, **40**, 1584-1589**.**
50. T. Sandmeyer, *Eur. J. Inorg. Chem*., 1884, **17**, 2650-2653.
51. Q. Wen, J. Jin, L. Zhang, Y. Luo, P. Lu and Y. Wang, *Tetrahedron Lett*., 2014, **55**, 1271-1280.
52. P. Anbarasan, T. Schareina and M. Beller, *Chem. Soc. Rev*., 2011, **40**, 5049-5067.
53. A. M. Nauth and T. Opatz, *Org. Biomol. Chem*., 2019, **17**, 11-23.
54. G. Yan, Y. Zhang and J. Wang, *Adv. Synth. Catal*., 2017, 359, 4068-4105.
55. T. Schareina, R. Jackstell, T. Schulz, A. Zapf, A. Cotte, M. Gotta and M. Beller, *Adv. Synth. Catal*., 2009, **351**, 643-648.
56. P. Puthiaraj, Pillaiyar, K. Yu, S. E. Shim and W. S. Ahn, *Mol. Catal*., 2019, **473**, 110395.
57. D. Ganapathy, S. S. Kotha and G. Sekar, *Tetrahedron Lett*., 2015, **56**, 175-178.
58. S. Sobhani, A. Habibollahi and Z. Zeraatkar, *Org. Process Res. Dev*., 2019, **23**, 1321-1332.
59. S. Sobhani, H. H. Moghadam, J. Skibsted and J. M. Sansano, *Green Chem*., 2020, **22**, 1353-1365.
60. S. Sobhani and Z. Ramezani, *RSC Adv*., 2016, **6**, 29237-29244.
61. S. Sobhani, F. O. Chahkamali and J. M. Sansano, *RSC Adv*., 2019, **9**, 1362-1372.
62. S. Sobhani, M. S. Ghasemzadeh and M. Honarmand, *Catal. Lett*., 2014, **144**, 1515-1523.
63. M. Zhao, Y. Cao, X. Liu, J. Deng, D. Li and H. Gu, *Nanoscale Res. Lett*., 2014, **9**, 142.
64. S. S. Shinde, A. Sami and J. H. Lee, *J. Mater. Chem. A*, 2015, **3**, 12810-12819.
65. B. L. A. Prabhavathi Devi, K. Vijaya Lakshmi, K. N. Gangadhar, R. B. N. Prasad, P. S. Sai Prasad, B. Jagannadh and C. Narayana, *ChemistrySelect*, 2017, **2**, 1925-1931.
66. T. Begum, M. Mondal, M. P. Borpuzari, R. Kar, G. Kalita, P. K. Gogoi and U. Bora, *Dalton Trans*., 2017, **46**, 539-546.
67. J. Hannah, W. V. Ruyle, H. Jones, A. R. Matzuk, K. W. Kelly, B. E. Witzel and T. Y. Shen, *J. Med. Chem*., 1978, **21**, 1093-1100.
68. D. A. Horton, G. T. Bourne and M. L. Smythe, *Chem. Rev*., 2003, **103**, 893-930.
69. C. C. C. Johansson Seechurn, M. O. Kitching, T. J. Colacot and V. Snieckus, *Angew. Chem. Int. Ed*., 2012, **51**, 5062-5085.
70. D. Alberico, M. E. Scott and M. Lautens, *Chem. Rev*., 2007, **107**, 174-238.
71. J. Y. Lee and G. C. Fu, *J. Am. Chem. Soc*., 2003, **125**, 5616-5617.
72. J. Hamdi, A. A. Blanco, B. Diehl, J. B. Wiley and M. L. Trudell, *Org. Lett*., 2019, **21**, 3471-3475.
73. F. F. Fleming, L. Yao, P. C. Ravikumar, L. Funk and B. C. Shook, *J. Med. Chem*., 2010, **53**, 7902-7917.
74. L. H. Jones, N. W. Summerhill, N. A. Swain and J. E. Mills, *MedChemComm*., 2010, **1**, 309-318.
75. V. Kandathil, A. Siddiqa, A. Patra, B. Kulkarni, M. Kempasiddaiah, B. S. Sasidhar, and S. A. Patil, Appl. Organomet. Chem., 2020, 34, e5924.
76. T. Begum, M. Mondal, M. P. Borpuzari, R. Kar, G. Kalita, P. K. Gogoi, and U. Bora, *Dalton Trans.,* 2017, **46**, 539-546.
77. H. Veisi, *Polyhedron*, 2019, **159**, 212-216.
78. S. Rostamnia, H. G. Hossieni and E, Doustkhah, *J. Organomet. Chem*., 2015, **791**, 18-23.
79. K. Karami, N. Jamshidian, M. M. Nikazma, P. Herves, A. R. Shahreza and A. Karami, *Appl. Organomet. Chem*., 2018, **32**, e3978.
80. B. Sreedhar, A. S. Kumar and D. Yada, *Synlett*, 2011, **8**, 1081-1084.
81. M. M. Amini, A. Mohammadkhani and A. Bazgir, *ChemistrySelect*, 2018, **3**, 1439-1444.
82. A. Ohtaka, Atsushi, T. Kotera, A. Sakon, K. Ueda, G. Hamasaka, Y. Uozumi and R. Nomura, *Synlett*, 2016, **27**, 1202-1206.

83. M, Esmaeilpour, A. R. Sardarian and H. Firouzabadi, *J. Organomet. Chem*., 2018, **873**, 22-34.
84. Y. Qian, J. So, S. Y. Jung, S. Hwang, M. J. Jin and S. E. Shim, *Synthesis*, 2019, **51**, 2287-2292.
85. S. Shabbir, S. Lee, M. Lim, H. Lee, H. Ko, Y. Lee and H. Rhee, *J. Organomet. Chem*., 2017, **846**, 296-304.
86. V. Kandathil, T. S. Koley, K. Manjunatha, R. B. Dateer, R. S. Keri, B. S. Sasidhar and S. A. Patil, *Inorganica Chim. Acta*, 2018, **478**, 195-210.
87. J. H. Park, F. Raza, S. J. Jeon, H. I. Kim, T. W. Kang, D. Yim and J. H. Kim, *Tetrahedron Lett*., 2014, **55**, 3426-3430.
88. V. Kandathil, B. D. Fahlman, B. S. Sasidhar, S. A. Patil and S. A. Patil, *New J. Chem*., 2017, **41**, 9531-9545.
89. H. Veisi, S. Najafi and S. Hemmati, *Int. J. Biol. Macromol.*, 2018, **113**, 186-194.
90. J. Chen, J. Zhang, Y. Zhang, M. Xie and T. Li, *Appl. Organomet. Chem*., 2020, **34**, e5310.
91. S. K. Dangolani, S. Sharifat, F. Panahi and A. Khalafi-Nezhad, *Inorganica Chim. Acta*, 2019, **494**, 256-265.
92. G. Chen, J. Weng, Z. Zheng, X. Zhu, Y. Cai, J. Cai and Y. Wan, *Eur. J. Org. Chem*., 2008, **2008**, 3524-3528.
93. S. Velmathi and N. E. Leadbeater, *Tetrahedron Lett*., 2008, **49**, 4693-4694.
94. P. Y. Yeung, C. P. Tsang and F. Y. Kwong, *Tetrahedron Lett*. 2011, **52**, 7038-7041.

Supplementary Information

Water-dispersible Pd-*N*-heterocyclic carbene complex immobilized on magnetic nanoparticles as a new heterogeneous catalyst for fluoride-free Hiyama, Suzuki and cyanation reactions in aqueous media

Farhad Omarzehi Chahkamali,[a] Sara Sobhani[a]* and José Miguel Sansano[b]

Address: [a] Department of Chemistry, College of Sciences, University of Birjand, Birjand, Iran. Fax: +98 56 32202065; Tel: +98 56 32202065; E-mail: ssobhani@birjand.ac.ir, sobhanisara@yahoo.com

[b] Departamento de Química Orgánica, Facultad de Ciencias, Centro de Innovación en Química Avanzada (ORFEO-CINQA) and Instituto de Síntesis Orgánica (ISO), Universidad de Alicante, Apdo. 99, 03080-Alicante, Spain.

General information

Chemicals were purchased from Merck Chemical Company. NMR spectra were recorded in ppm in $CDCl_3$ and DMSO-d_6 using a Bruker Advance DPX-300 instrument with TMS as the internal standard.

Spectral Data:

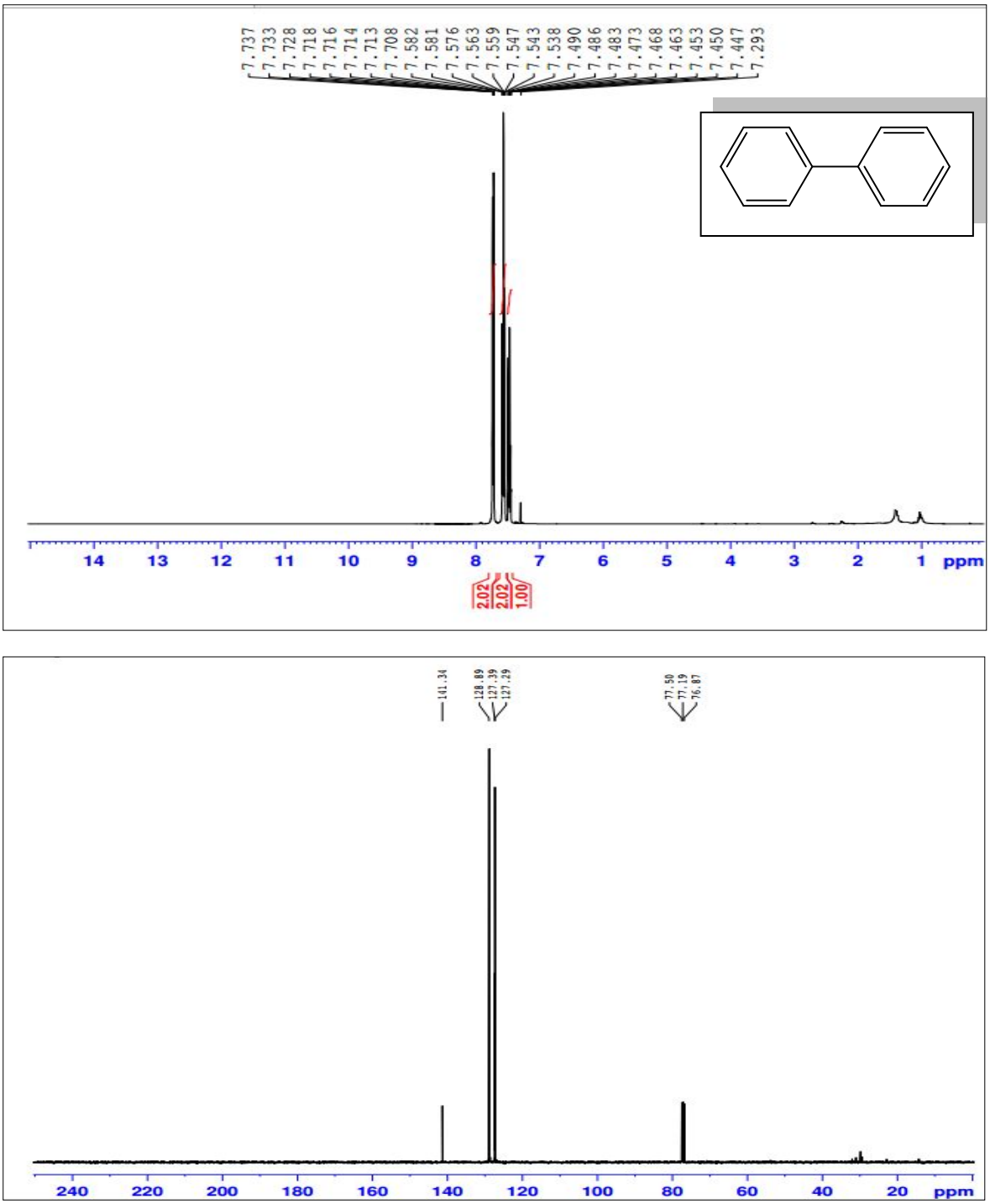

Figure S1. ^{1}H NMR and ^{13}C NMR spectra of biphenyl **1** (Table 1 and 2: entries 1, 5 and 9) ^{1}H NMR (300 MHz, $CDCl_3$): δ 7.46 (t, ^{3}J = 7.2 Hz, 2 H), 7.56 (t, ^{3}J = 8.0 Hz, 4 H,), δ 7.72 (d, ^{3}J = 6.8 Hz, 4 H) ppm; ^{13}C NMR (100 MHz, $CDCl_3$): δ 127.2, 127.3, 128.8, 141.3 ppm.

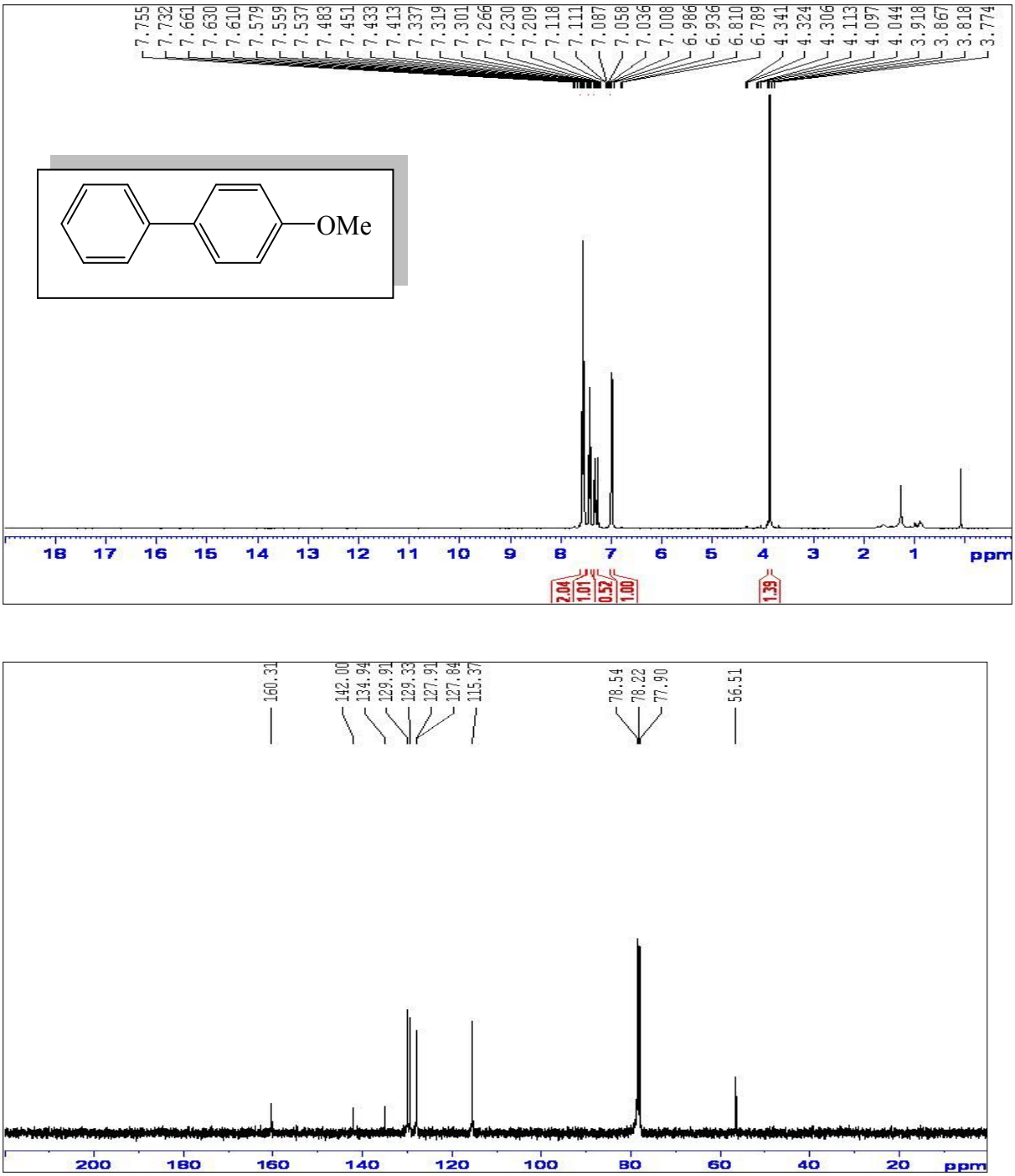

Figure S2. ^{1}H NMR and ^{13}C NMR spectra of 4-methoxybiphenyl **2** (Table 1 and 2: entries 2 and 6)

^{1}H NMR (300 MHz, $CDCl_3$): δ 3.83 (s, 3 H), 6.99 (d, ^{3}J = 8.8 Hz, 2 H), 7.31 (t, ^{3}J = 7.2 Hz, 1 H), 7.43 (t, ^{3}J = 8.0 Hz, 2 H), 7.55 (t, ^{3}J = 8.8 Hz, 4 H) ppm; ^{13}C NMR (100 MHz, $CDCl_3$): δ 56.5, 115.3, 127.8, 127.9, 129.3, 129.9, 134.9, 142.0, 160.3 ppm.

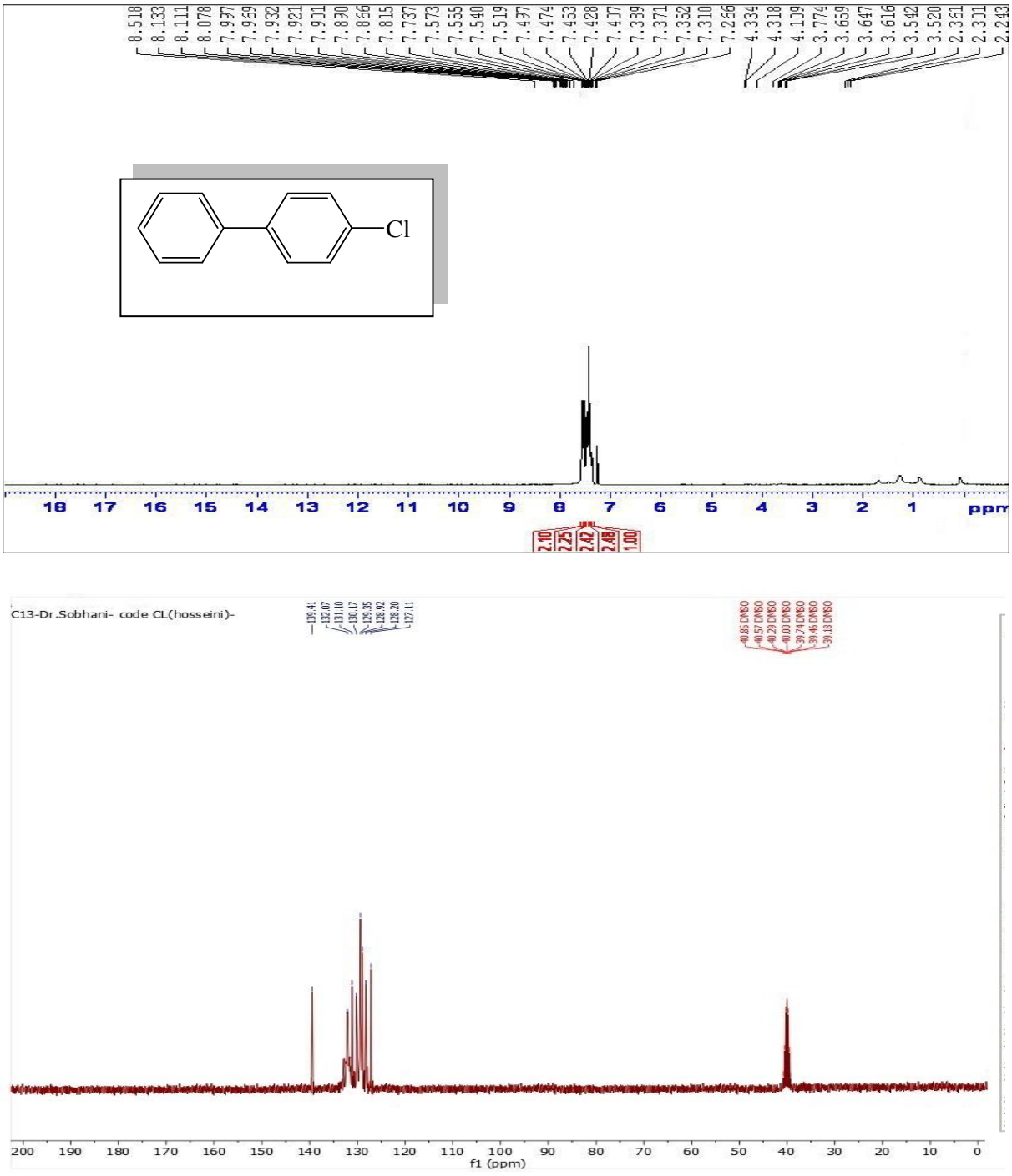

Figure S3. ^{1}H NMR and ^{13}C NMR spectra of 4-chlorobiphenyl **3** (Table 1 and 2: entries 3 and 7)

^{1}H NMR (300 MHz, $CDCl_3$): δ 7.31-7.49 (m, 5 H), 7.51-7.57 (m, 4 H) ppm; ^{13}C NMR (100 MHz, DMSO-d6): δ 127.1, 128.2, 128.9, 129.3, 130.1, 131.1, 132.0, 139.4 ppm.

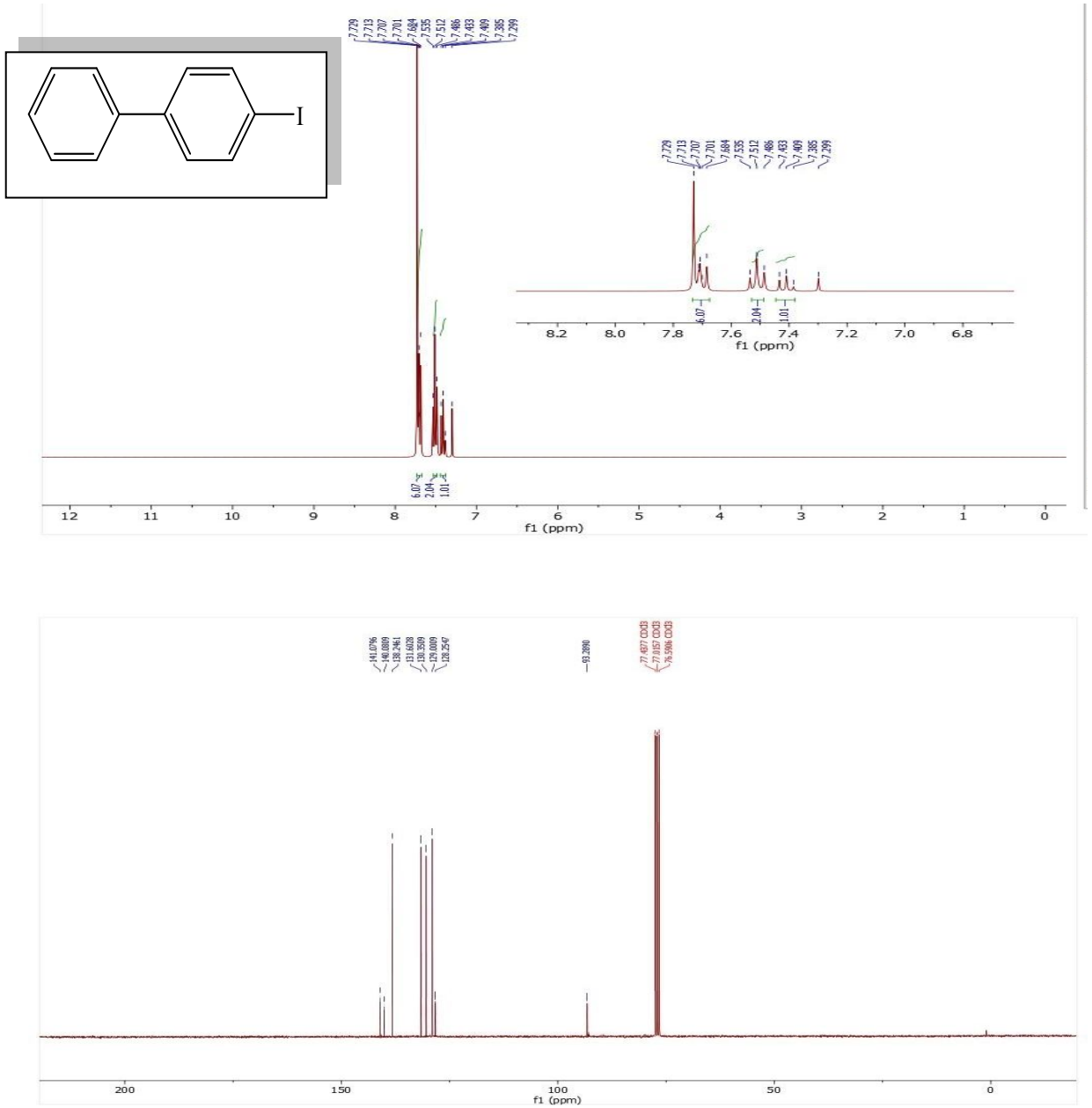

Figure S4. ^{1}H NMR and ^{13}C NMR spectra of 4-iodo-1,1'-biphenyl **4** (Table 1 and 2: entry 4) ^{1}H NMR (300 MHz, $CDCl_3$): δ 7.40 (t, ^{3}J = 7.2 Hz, 1 H), 7.51 (t, ^{3}J = 7.8 Hz, 2 H), 7.67-7.73 (m, 6 H) ppm; ^{13}C NMR (75 MHz, $CDCl_3$): δ 93.2, 128.2, 129.0, 130.3, 131.6, 138.2, 140.0, 141.0 ppm.

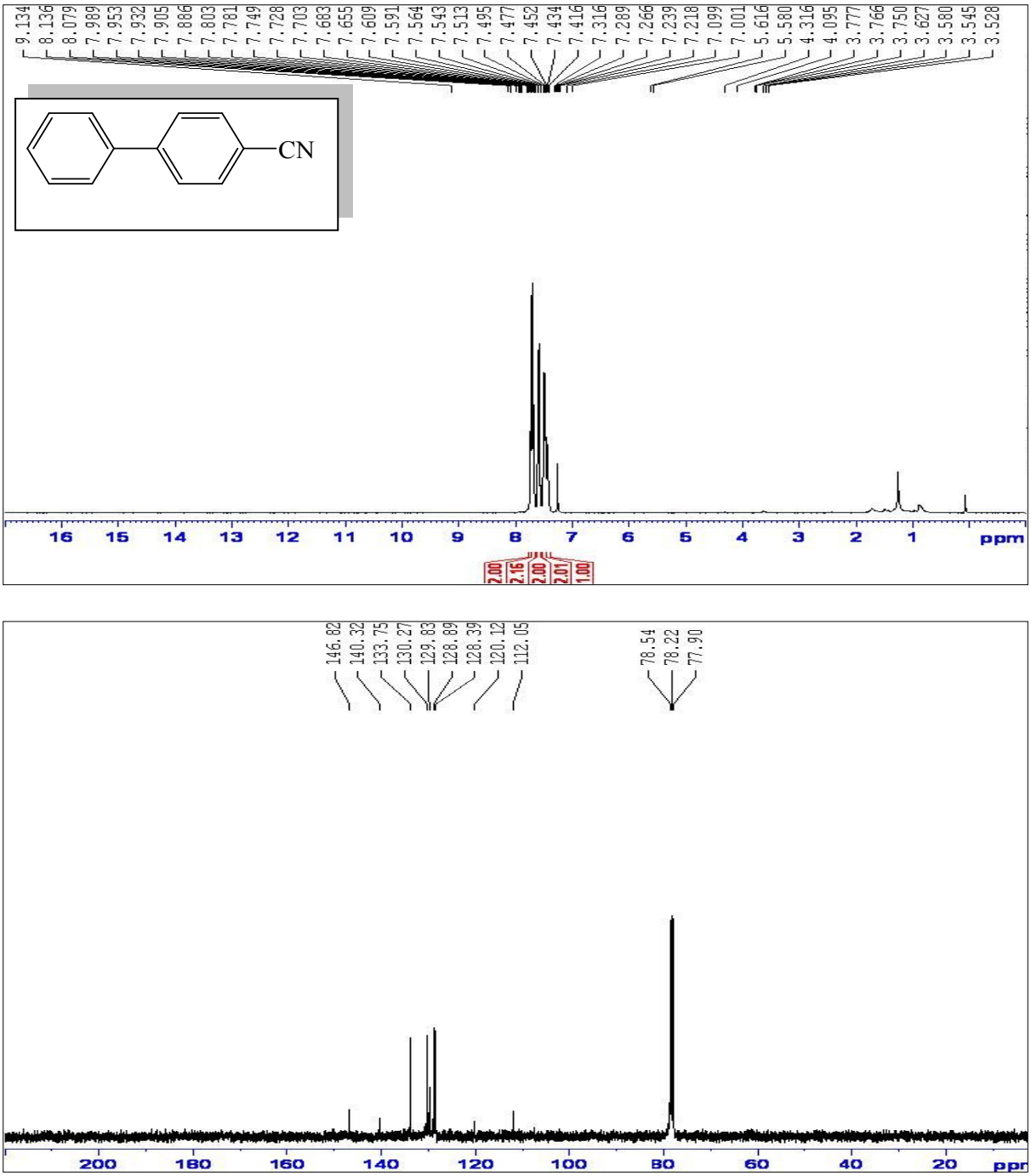

Figure S5. ^{1}H NMR and ^{13}C NMR spectra of 4-cyanobiphenyl **5** (Table 1 and 2: entries 8 and 11)

^{1}H NMR (300 MHz, $CDCl_3$): δ 7.41-7.51 (m, 3 H), 7.56-7.60 (m, 2 H), 7.68-7.74 (m, 4 H) ppm.; ^{13}C NMR (100 MHz, $CDCl_3$): δ 112.0, 120.1, 128.3, 128.8, 129.8, 130.2, 133.7, 140.3, 146.8 ppm.

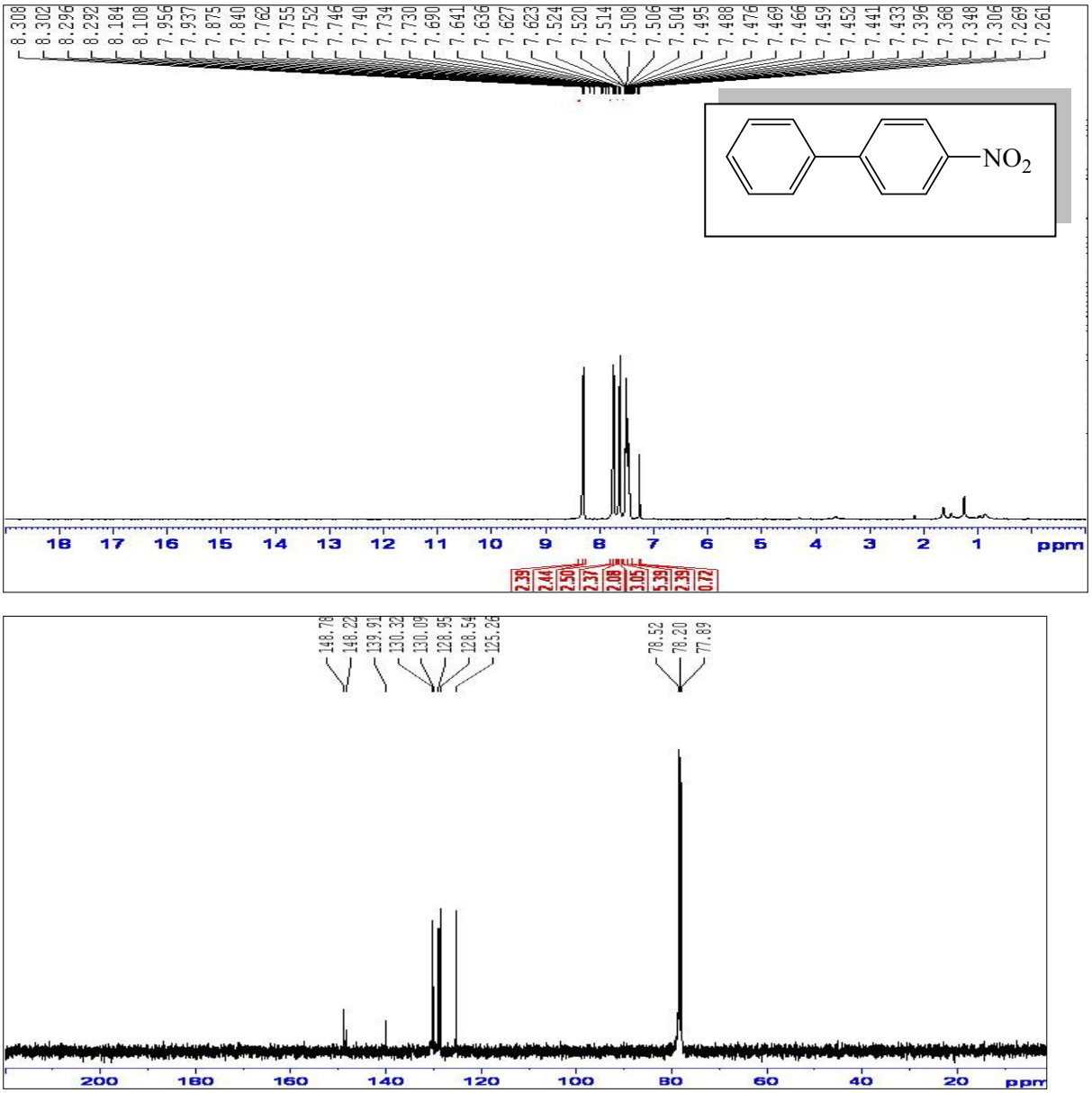

Figure S6. ^{1}H NMR and ^{13}C NMR spectra of 4-nitrobiphenyl **6** (Table 1 and 2: entry 10) ^{1}H NMR (300 MHz, $CDCl_3$): δ 7.43-7.52 (m, 3 H), 7.62-7.64 (m, 2 H), 7.73-7.76 (m, 2 H), 8.29-8.30 (m, 2 H) ppm; ^{13}C NMR (100 MHz, $CDCl_3$): δ 125.2, 128.5, 128.9, 130.0, 130.3, 139.9, 148.2, 148.7 ppm.

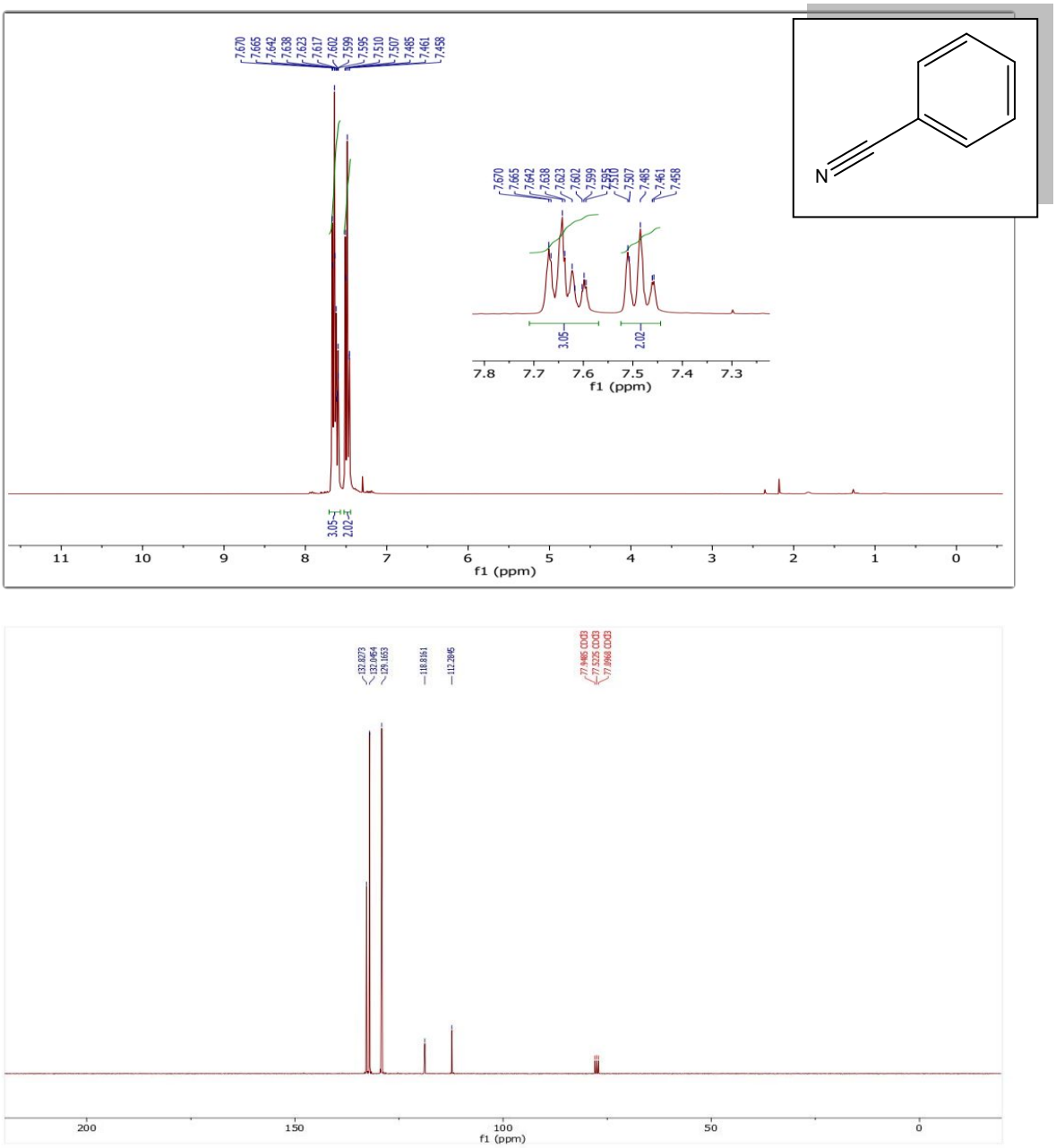

Figure S7. ^{1}H NMR and ^{13}C NMR spectra of benzonitrile **7** (Table 3: entries 1,5,13 and 18) ^{1}H NMR (300 MHz, $CDCl_3$); δ 7.48 (t, J = 7.8 Hz, 2 H), 7.59-7.67 (m, 3 H) ppm; ^{13}C NMR (75 MHz, CDCl3): δ 112.2, 118.8, 129.1, 132.0, 132.8 ppm.

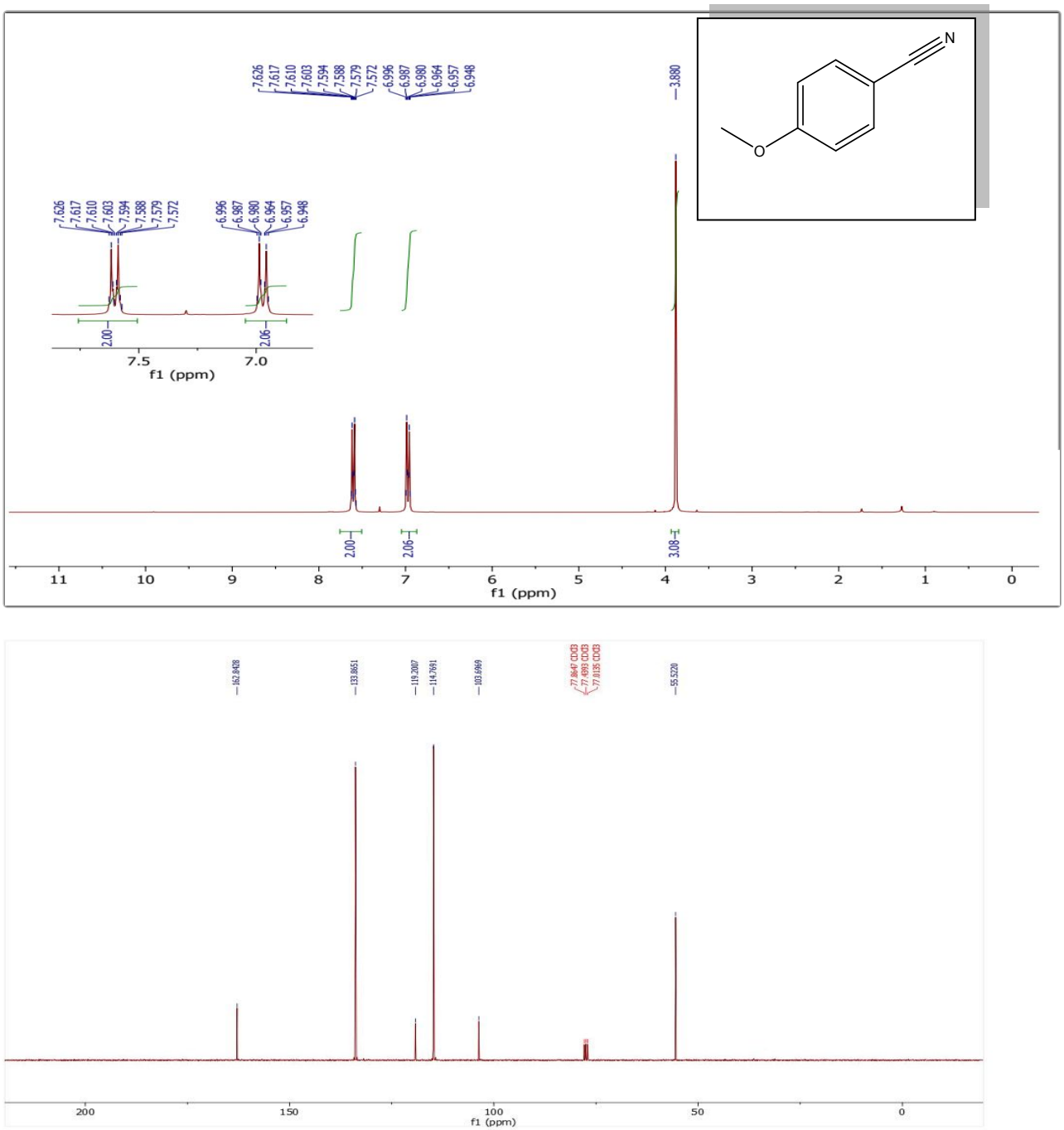

Figure S8. ^{1}H NMR and ^{13}C NMR spectra of 4-methoxybenzonitrile **8** (Table 3: entries 2 and 7)

^{1}H NMR (300 MHz, $CDCl_3$); δ 3.88 (s, 3 H), 6.97 (d, J = 9 Hz, 2 H), 7.60 (d, J = 9 Hz, 2 H) ppm; ^{13}C NMR (75 MHz, $CDCl_3$): δ 55.5, 103.6, 114.7, 119.2, 133.8, 162.8 ppm.

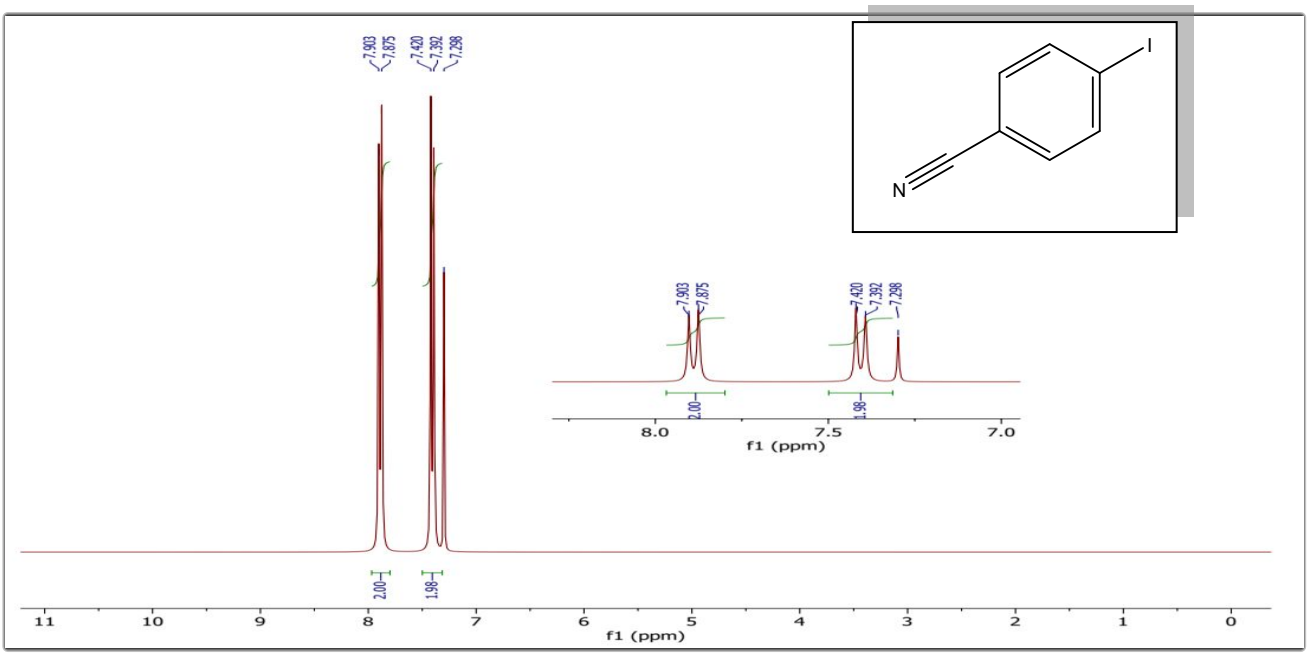

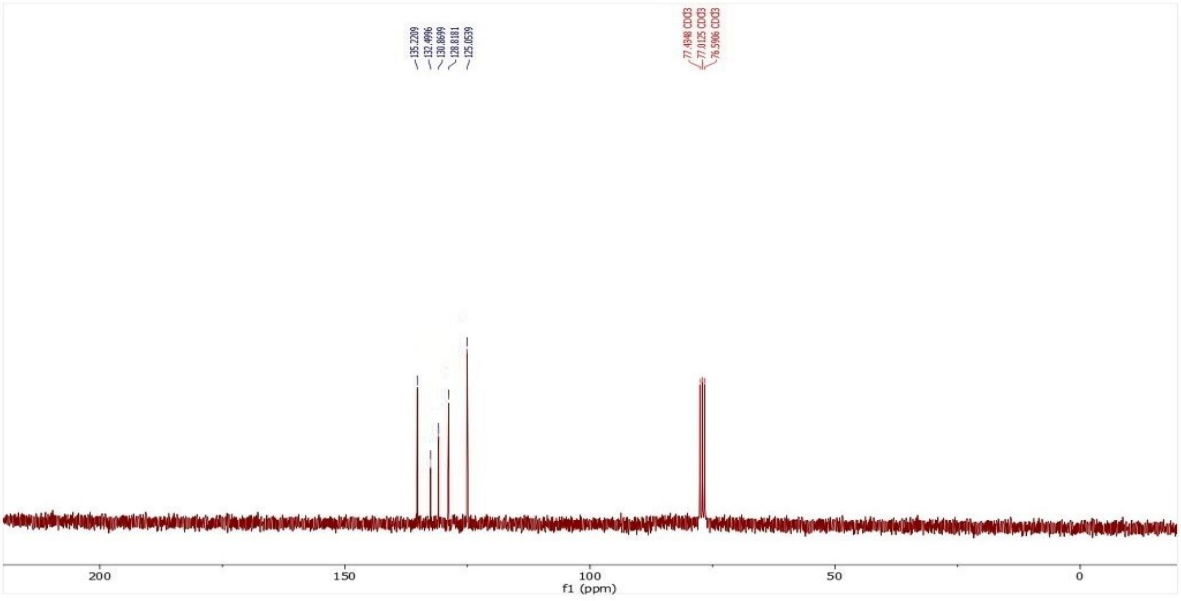

Figure S9. ^{1}H NMR and ^{13}C NMR spectra of 4-iodobenzonitrile **9** (Table 3: entry 3) ^{1}H NMR (300 MHz, $CDCl_3$); δ 7.40 (d, J = 8.4 Hz, 2 H), 7.89 (d, J = 8.4 Hz, 2 H) ppm; ^{13}C NMR (75 MHz, $CDCl_3$): δ 125.0, 128.8, 130.8, 132.4, 135.2 ppm.

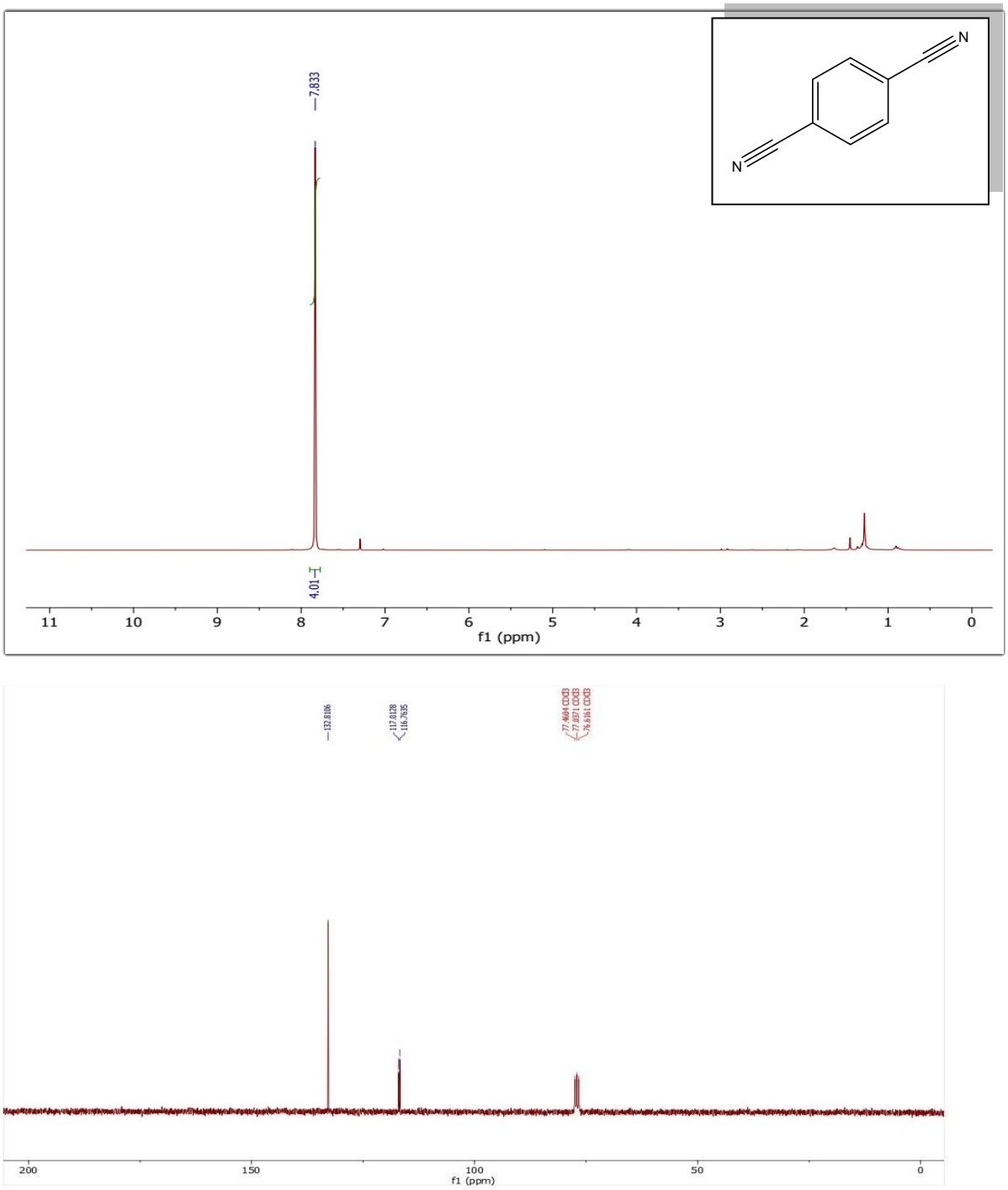

Figure S10. ^{1}H NMR and ^{13}C NMR spectra of terephthalonitrile **10** (Table 3: entries 4, 8, 11 and 16)

^{1}H NMR (300 MHz, $CDCl_3$); δ 7.83 (s, 4 H) ppm; ^{13}C NMR (75 MHz, $CDCl_3$): δ 116.7, 117.0, 132.8 ppm.

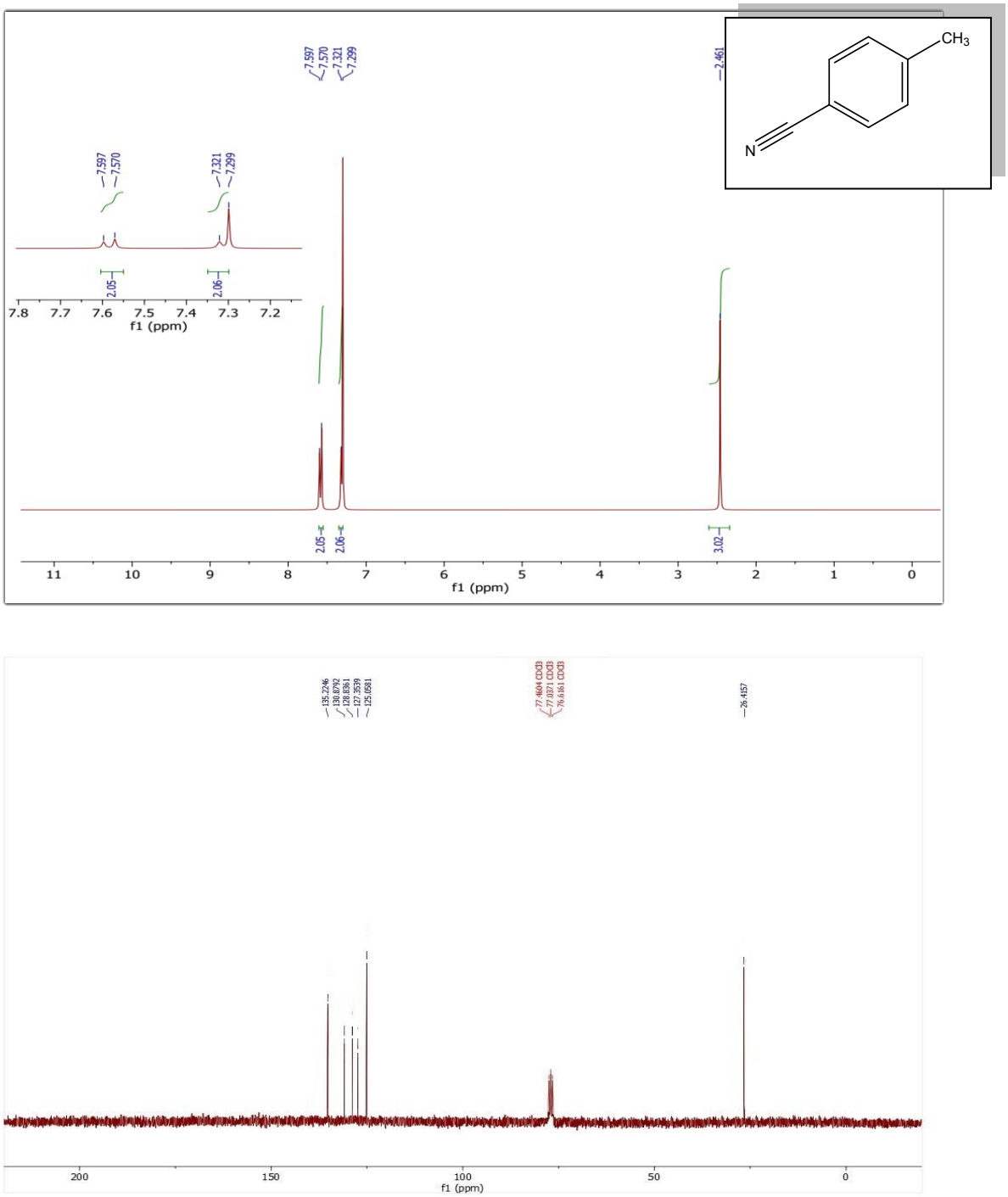

Figure S11. ^{1}H NMR and ^{13}C NMR spectra of 4-methylbenzonitrile **11** (Table 3: entries 6 and 14)

^{1}H NMR (300 MHz, $CDCl_3$); δ 2.46 (s, 3 H), 7.31 (d, J = 6.6 Hz, 2 H), 7.58 (d, J = 8.1 Hz, 2 H) ppm; ^{13}C NMR (75 MHz, $CDCl_3$): δ 26.4, 125.0, 127.3, 128.8, 130.8, 135.2 ppm.

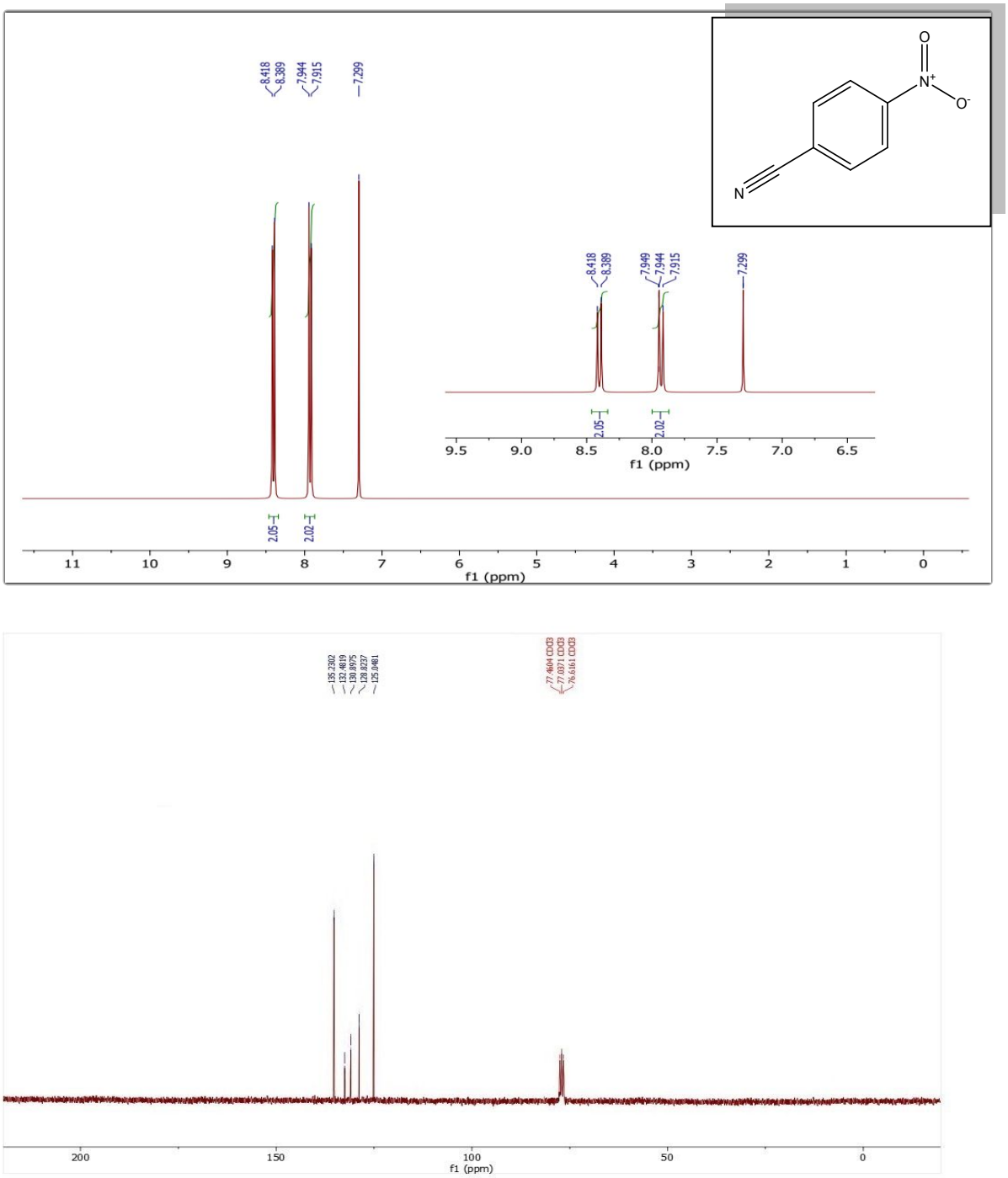

Figure S12. ^{1}H NMR and ^{13}C NMR spectra of 4-nitrobenzonitrile **12** (Table 3: entries 9 and 15)

^{1}HNMR (300 MHz, $CDCl_3$); δ 7.92 (d, J = 8.7 Hz, 2 H), 8.40 (d, J = 8.7 Hz, 2 H) ppm; ^{13}C NMR (75 MHz, $CDCl_3$): δ 125.0, 128.8, 130.8, 132.4, 135.2 ppm.

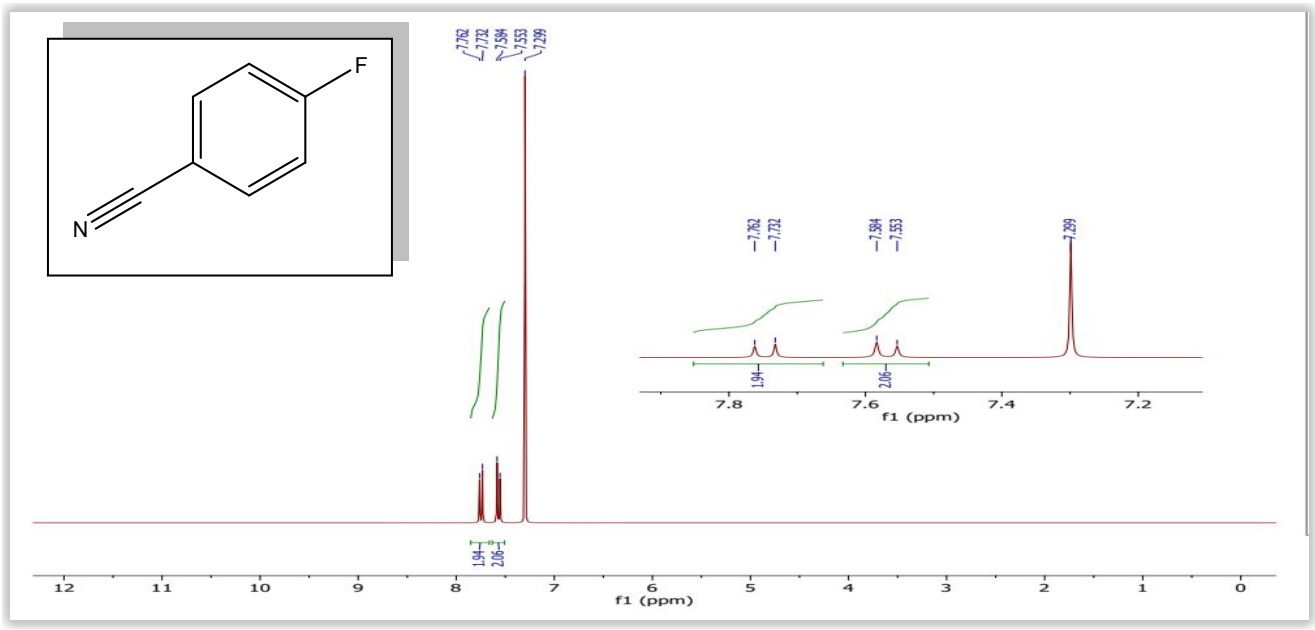

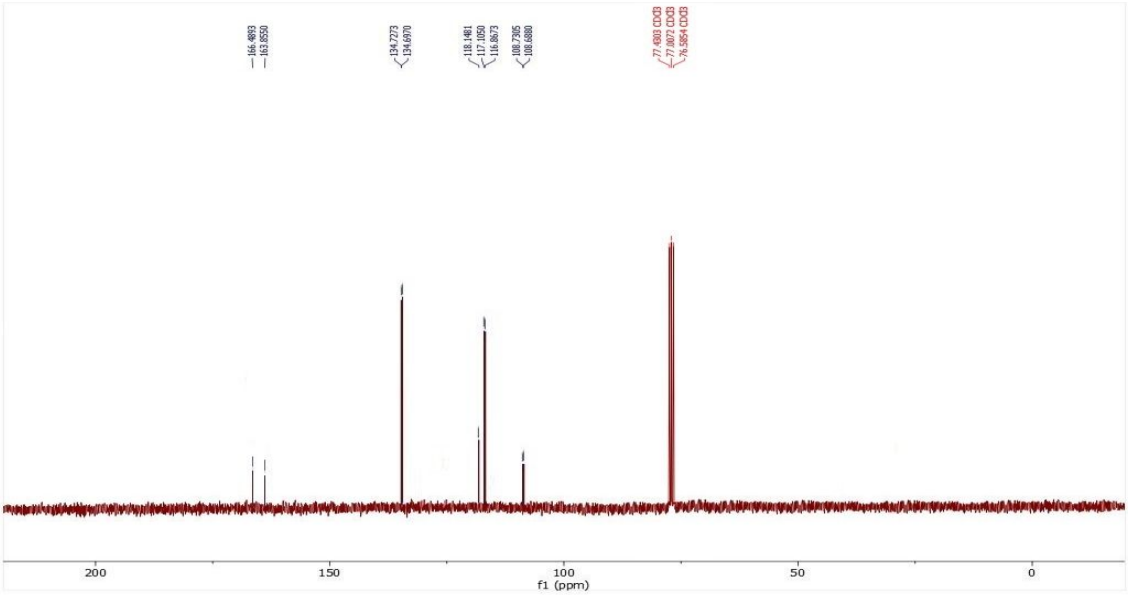

Figure S13. ^{1}H NMR and ^{13}C NMR spectra of 4-fluorobenzonitrile **13** (Table 3: entry 10) ^{1}H NMR (300 MHz, $CDCl_3$); δ 7.56 (d, J = 9.3 Hz, 2 H), 7.74 (d, J = 9 Hz, 2 H) ppm; ^{13}C NMR (75 MHz, $CDCl_3$): δ 108.6 (d, $J_{C\text{-}F}$= 3.7 Hz), 116.9 (d, $J_{C\text{-}F}$= 22.5 Hz), 118.1, 134.6 (d, $J_{C\text{-}F}$= 7.5 Hz), 165.1 (d, $J_{C\text{-}F}$= 195 Hz) ppm.

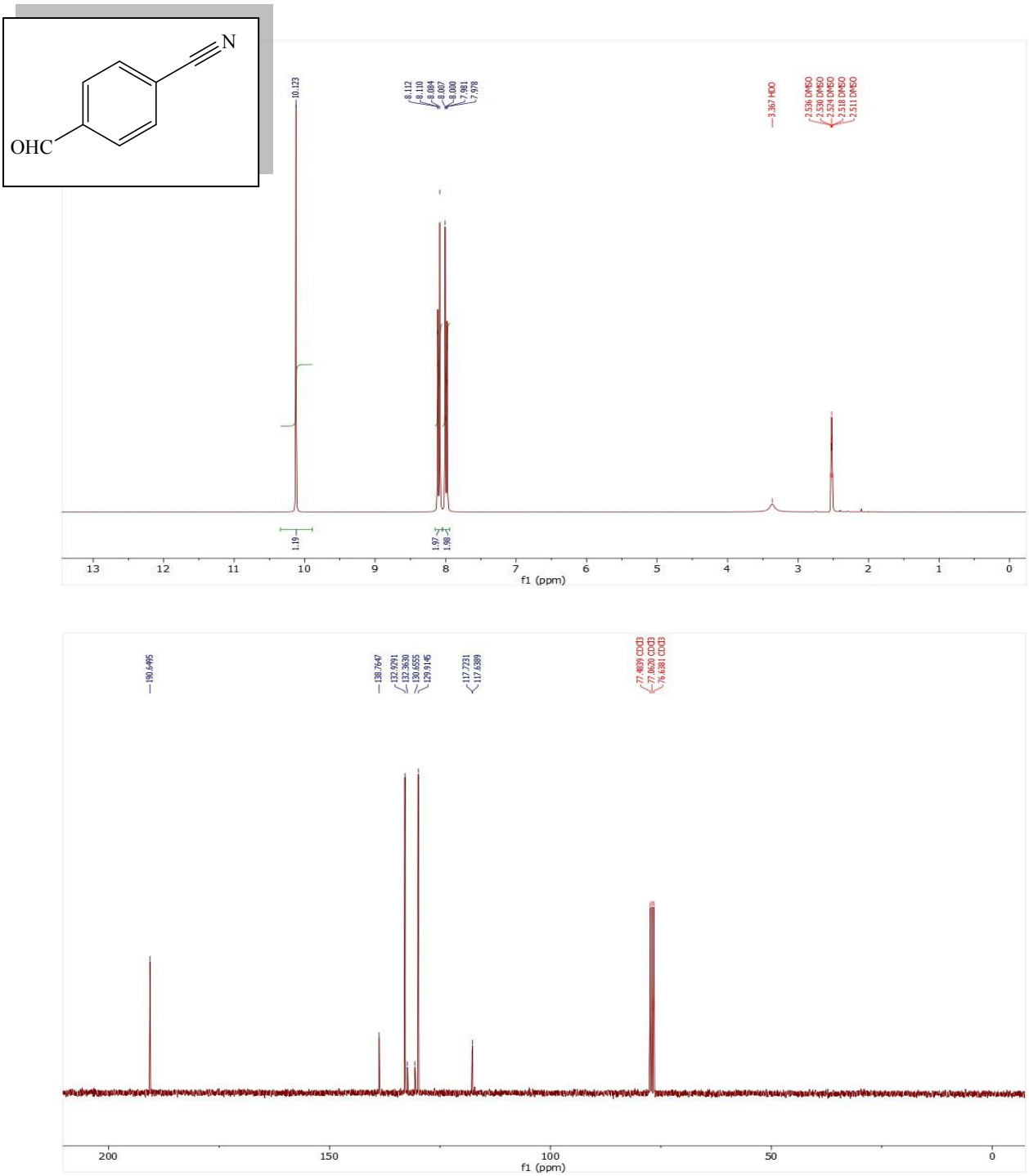

Figure S14. ^{1}H NMR and ^{13}C NMR spectra of 4-cyanobenzaldehyde **14** (Table 3: entries 12 and 17)

^{1}H NMR (300 MHz, DMSO-d_6); δ 7.99 (d, J = 7.8, 2 H), 8.09 (d, J = 7.8, 2 H), 10.12 (s, 1 H) ppm; ^{13}C NMR (75 MHz, $CDCl_3$), δ 117.7, 129.9, 132.9, 138.7, 190.6 ppm.

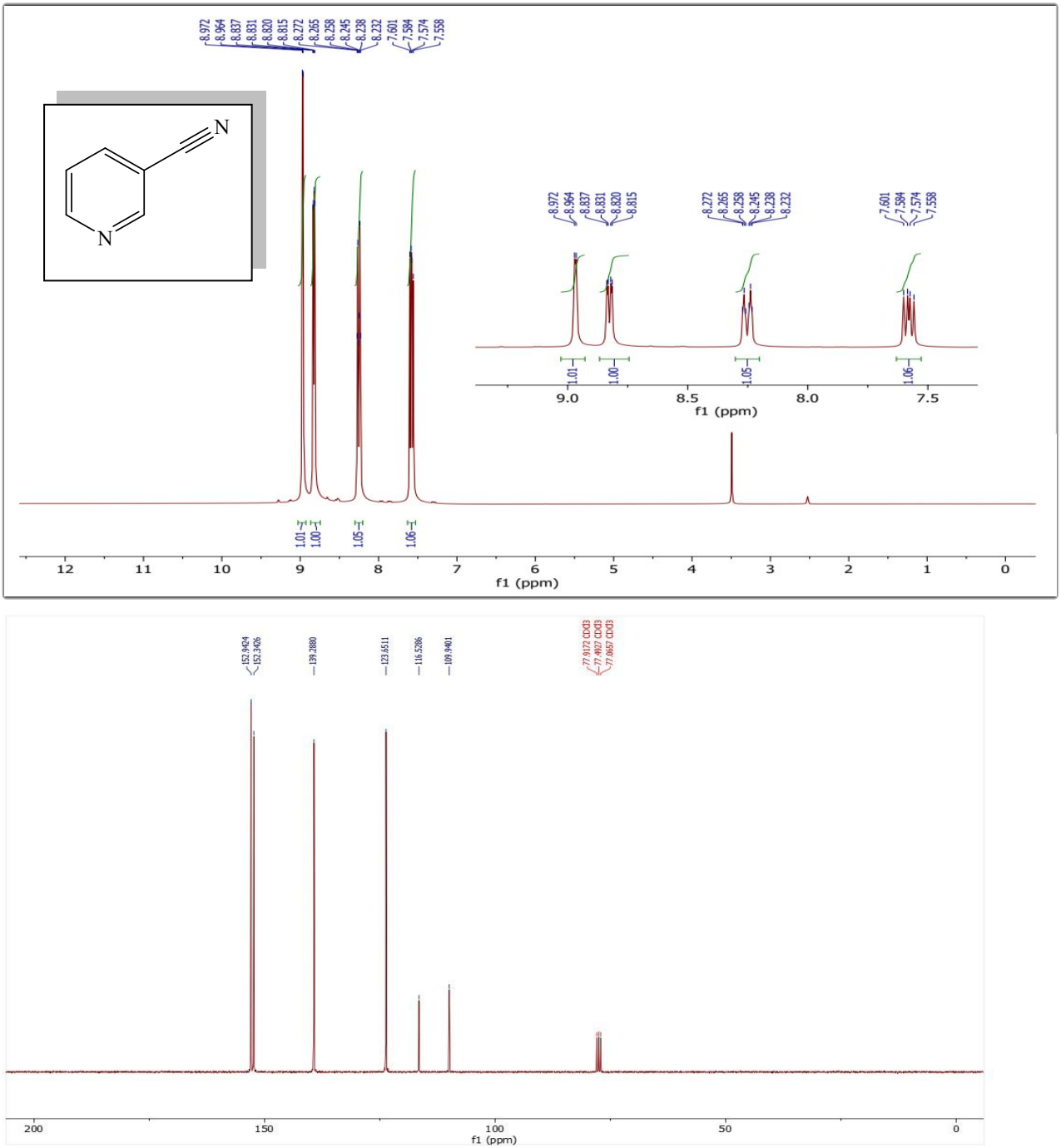

Figure S15. ^{1}H NMR and ^{13}C NMR spectra of nicotinonitrile **15** (Scheme 3)

^{1}H NMR (300 MHz, DMSO-d_6); δ 7.56-7.60 (m, 1 H), 8.25 (d, J = 8.1 Hz, 1 H), 8.82 (d, J = 5.1 Hz, 1 H), 8.96 (s, 1 H) ppm; ^{13}C NMR (75 MHz, $CDCl_3$): δ 109.9, 116.5, 123.6, 139.2, 152.3, 152.9 ppm.

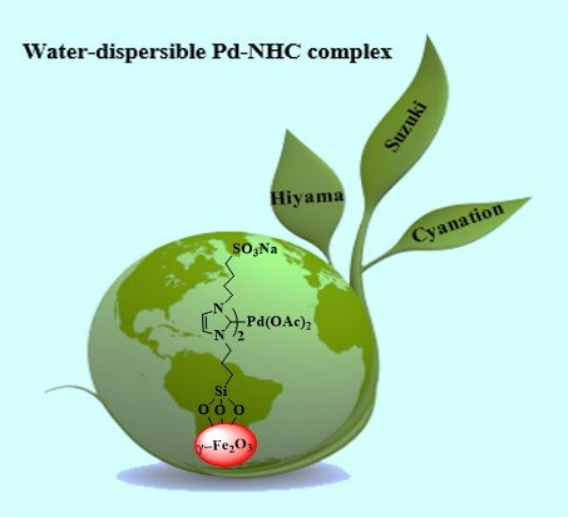

A new nanomagnetic water-dispersible Pd-*N*-heterocyclic carbene complex as a catalyst for the C-C coupling reactions in water is introduced.

Statement

Although a plethora of biochemical reactions occurs in aqueous media, a very small percentage of synthetic organic reactions are carried out in aqueous media. The reasons for the historical restricted use of water as the reaction medium may be related to two main reasons: the first is the hydrophobic effect which severely limits the solubility of nonpolar organic materials and the second is the instability of organometallic complexes in aqueous media. This important drawback is also the main reason why most of the reactions that are carried out in water include also a co-solvent or phase transfer agent to improve solubility. Although, water often considered as the "natural enemy" of organometallic species, Breslow was proposed the first *N*-heterocyclic carbene (NHC) catalysis in the aqueous media. Thermal and chemical stabilities of NHC catalysts in the moisture and air are due to the strong NHC-metal bonds, which originates from strong σ-donor and low σ-acceptor abilities of these ligands.

Despite the wide application of the homogeneous Pd-NHC catalysts in organic transformations, their recycling is very complicated because their separation is extremely difficult. One way to overcome this drawback is the immobilization of Pd-NHC on different solid supports. Within the solid supports, MNPs provide an easy catalyst isolation by a magnetic separation method using an external magnet. Magnetic separation, which is an alternative to filtration or centrifugation, prevents loss of the catalyst, and saves time and energy. However, one significant limitation of using MNPs is that they are readily aggregated when suspended in the solvent due to the self-interactions. Surfactants with relatively high concentrations are often required to prevent such an aggregation in water. A more desirable approach, which avoids using any additives, is designing water-dispersible MNPs. This allows reactions to be performed in pure water under near homogeneous conditions. Although preparation of water dispersible MNPs through surface modification with hydrophilic groups have been pursued by many research groups for bio-related applications, there are few articles on the synthesis of magnetically recyclable water-dispersible catalysts and their applications in organic transformations in neat water. Therefore, there is still much room for developing new magnetically recyclable water-dispersible catalysts in pure aqueous media.

In this paper, we have synthesized a novel water-dispersible Pd-N-heterocyclic carben complex immobilized on magnetic nanoparticles (γ-Fe_2O_3-Pd-NHC-*n*-butyl-SO_3Na) and characterized it by different methods such as FT-IR, XPS, EDX, TEM, FESEM, TGA, VSM and ICP analysis. The synthesized catalyst was used as a new water dispersible heterogeneous catalyst in the fluoride-free Hiyama, Suzuki and cyanation reactions. By this method, different types of biphenyls and aryl nitriles were synthesized in good to high yields by the reaction of a variety of aryl iodides, bromides and chlorides with triethoxyphenylsilane, phenylboronic acid and $K_4[Fe(CN)_6]\cdot 3H_2O$ in pure water without using any additives and co-solvent. The presence of sulfonates as hydrophilic groups on the surface of the catalyst generates a stable dispersion of the catalyst in water as the reaction medium and exposes the active palladium sites to substrates like homogeneous systems, thus increasing the catalytic activity. The catalyst exhibited extremely low solubility in organic solvents. Using this property, the recovered aqueous phase containing the catalyst was simply and efficiently used in seven consecutive runs without a significant decrease in activity. At the end of the process the catalyst was easily isolated from the aqueous phase by using an external magnetic field. Hot filtration and poisoning tests indicate that the catalytic reaction is mainly heterogeneous in nature. A plausible mechanism for the catalytic cycle of Hiyama, Suzuki and cyanation reactions are also proposed. The possibility to perform the reaction in water as a green medium, easy catalyst recovery and reuse by successive extraction and final magnetic separation, and not requiring any additive or co-solvent make this method a valid candidate for the synthesis of biphenyl derivatives and aryl nitriles.